Centre for Geo-Information

Thesis Report GIRS-2012-07

LARGE AREA LAND COVER CLASSIFICATION USING MULTI-YEAR SATELLITE DATA AND STABILITY TEST

A case study of Mato Grosso, Brazil

Ugbaje Sabastine Ugbemuna

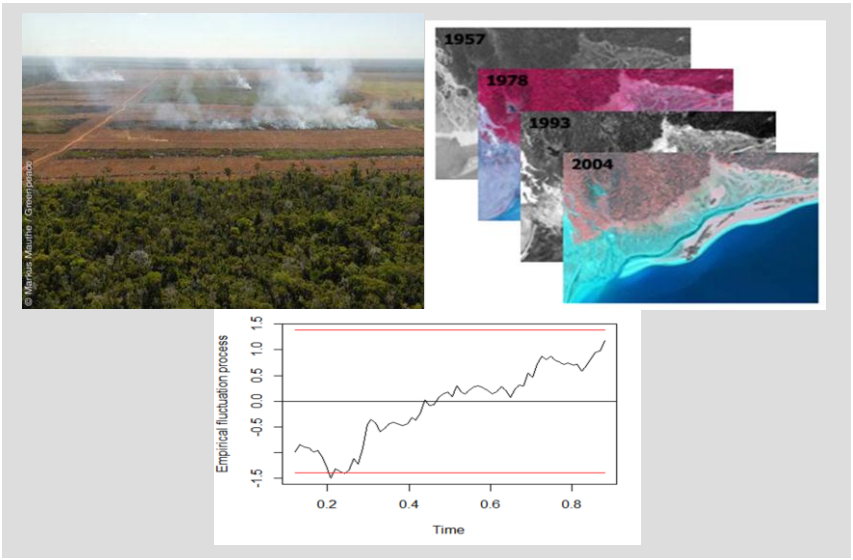

MAY 2012

WAGENINGEN UNIVERSITY
WAGENINGEN UR

Large area land cover classification using multi-year satellite data and stability test

A case study of Mato Grosso, Brazil

Ugbaje Sabastine Ugbemuna

791111847110

Supervisors:

Prof. Dr. M. Herold

Dr. J. Verbesselt

M. Kalomenopoulos, MSc

A thesis submitted in partial fulfilment of the degree of Master of Science

at Wageningen University and Research Centre,

The Netherlands.

May 2012

Wageningen, The Netherlands

Thesis code number: GRS-80436
Thesis Report: GIRS-2012-07
Wageningen University and Research Centre
Laboratory of Geo-Information Science and Remote Sensing

Table of Contents

Abstract

Reliable and accurate information on land cover is important for understanding the state and dynamics of the terrestrial ecosystem and the impact of climate change on the environment. Unfortunately, current global land cover products suffer from label instability as comparison between successive products show spurious changes not associated with changes in the *land cover state* (e.g. from forest to grassland). Conventional methods for global land cover classification use few instantaneous observations of the land cover state often from a single-year satellite data, thus making the products sensitive to intra- and inter-annual variation in the *land cover condition* (e.g. insect infestation of forest, temporal modification of grassland due to drought). We propose a method for land cover classification that uses multi-year satellite data and stability test to produce stable 'best' land cover map(s) (STBM) that should be less prone to variation in the *land cover condition.* Prior to land cover classification, the stability test is used to test the stability of the land cover over the observation period and separate stable pixels from unstable ones. Stable pixels are classified using the entire data and unstable pixels are classified using the latest year data; these are then combined to form the STBM. We tested our method using five years (2005-2009) 16-day Moderate Resolution Imaging Spectroradiometer (MODIS) composites acquired over a region encompassing almost the entire State of Mato Grosso in Brazil and extending marginally into Eastern Bolivia. Stability test was applied on the Enhanced Vegetation Index (EVI) time series, employed as a proxy indicator of the land cover state and condition. The STBM was classified into five classes: *Forest, Croplands and cropland/vegetation mosaics, Other vegetation and mosaics, Urban and barren, and Water*. We evaluated the STBM for classification accuracy and label stability. Result of the stability test showed that 24 % of the study area was unstable ($p < 0.05$). Except for the *Urban and barren class,* the overall and individual class (producer's and user's) accuracies of the STBM were high (> 80 %). STBM was compared with a baseline status map (BSLM, classified using 2005-2006 MODIS data) to extract areas that were possibly deforested over 2006 to 2009. Only 33.2 % of deforested areas captured in the deforestation records (PRODES) for the region was captured by STBM and BLSM comparison. Analysis with Breaks For Additive Seasonal and Trend (BFAST) method revealed that temporal disturbance events (e.g. fire, drought, selective logging) in some forest areas over the observation period were captured as deforestation by PRODES while STBM and BLSM comparison indicated no deforestation. Overall, the findings from this study demonstrate the potentials of our proposed approach to produce accurate land cover maps that would be less prone to the ever changing condition of land cover (e.g. from fire, drought). However, this approach needs to be further tested in other ecological regions of the world. Thematic legends as detailed as those used in the current global land cover products should be employed in the classification.

Keywords: land cover, classification, stability test, multi-year satellite data, land cover state, land cover condition, deforestation.

List of Figures

List of Tables

Acknowledgements

I wish to express my profound gratitude to my thesis supervisors, Prof. Dr. M. Herold, Dr. J. Verbesselt and Mr. M. Kalomenopoulos, for guiding me through the course of this thesis work. Their suggestions and constructive criticisms have greatly enriched this thesis and improved my research skills. To them I will always remain indebted.

Many thanks to my friend Eliakim for sharing in my excitements and challenges while this thesis lasted. I can never thank him enough! My appreciation also goes to Loïc and Wiecher for tips on data pre-processing and scripting in R.

Finally, I would like to thank Dr. C. Souza Jr. of IMAZON, Brazil for providing the PRODES data that was used in this thesis.

1 Introduction

1.1 Context and background

Land cover and land cover change are among the most obvious and commonly employed indicators of the state and dynamics of the terrestrial ecosystems driven by anthropogenic as well as natural processes (Herold et al., 2009;Hüttich et al., 2011). Land cover has been identified by the United Nations Framework Convention on Climate Change (UNFCCC) as one of eleven Essential Climate Variables (ECVs) that should be continuously monitored to reduce uncertainties in understanding the global climate system (GCOS, 2010;Herold et al., 2011), particularly as land cover is seen to be acting as both a cause and a consequence of climate change (Herold et al., 2009). Accurate and reliable information on land cover and land dynamics are critical for monitoring and understanding the anthropogenic and natural processes that impact and/or are impacted by climate change.

Remote sensing remains one of the primary means of mapping and characterising land cover and land cover change across a variety of spatiotemporal scales. A number of land cover mapping initiatives have been carried out at the national-, regional- and continental scale such as the Spanish Land Cover and Land Use Information System (Arozarena et al., 2006), the AfriCover maps (FAO, 2003) and the European Corine Land Cover databases (EEA, 2009, 2010a, b). The advent of moderate and high temporal resolution satellite sensors from the early 1990s has made mapping land cover at the global scale possible. The earliest global land cover maps derived from remote sensing data were made from the Advanced Very High-Resolution Radiometer (AVHRR, De Fries et al., 1998;Defries and Townshend, 1994). Since then, there have been quite a number of global land cover mapping efforts that have yielded land cover products in the 300 m - 1 km resolution range. The 1 km resolution land cover products include the IGPB- DISCover (Loveland et al., 2000), the UMD (Hansen et al., 2000), MODIS (Friedl et al., 2002), and the GLC2000 (Bartholomé and Belward, 2005). Other global land cover products are the 500 m resolution MODIS (Friedl et al., 2010) and the 300 m GlobeCover (Defourny et al., 2009). Although most of these products were more or less developed independently, comparison and interoperability between these products among the diverse community of modelling and land resource scientists is now possible following the wide acceptance of the Land Cover Classification Scheme (LCCS) of the Food and Agricultural Organization (FAO, Di Gregorio, 2005) as a universal standard for land cover characterization (Bontemps et al., 2011b;Herold et al., 2009). Although many applications that use land cover as proxy indicator of land surface characteristics rely on these land cover products, the existing land cover products have not fully met the needs and expectations of a number of research communities, particularly the Climate Modelling Community (CMC).

1.2 Problem definition

As one of the 11 ECVs, land cover data is of increasing importance for understanding the climate system, for assessing the impact of climate change, and for evolving mitigation strategies to reduce emissions to the atmosphere. For climate modelling land cover information is required to parameterize

land surface characteristics, such as vegetation fractional cover (VFC), surface roughness, leaf area index (LAI), albedo, and root depth (Ge et al., 2009) and/or used as validation datasets to evaluate model outcomes and to study feedback effects (Herold et al., 2011). Technological progress is increasingly making it easier to map land cover at previously unthinkable scale and speed, yet land cover characterization driven solely by advances in technology while ignoring user's needs will not fully benefit science and society (Herold et al., 2008b). Most of the available land cover products were produced for a broader range of applications, with little or no input from potential users. There is need for direct interactions between users and producers of land cover so as to understand their land cover information needs. Recently, the European Space Agency (ESA) has launched a Climate Change Initiative (CCI) programme that is aiming to provide adequate and comprehensive satellite-based products for monitoring the 11 ECVs, the land cover being one of them (ESA, 2009). One of the strategies of the CCI is to incorporate the needs of the users of these satellite-based products in the production process. As part of the CCI programme, a survey of the land cover information needs and requirements of the CMC was recently carried out and a number of key demands have been identified (Bontemps et al., 2011b).

One of the key demands of the CMC is 'stable land cover data and a dynamic component in form of time-series and changes in land cover' (Herold et al., 2011). A major problem with current land cover products is the temporal instability of land cover labels, even when this cannot be associated with land cover change. For example, Friedl et al. (2010) reported that about 31 % of the land surface was labelled differently between the MODIS 4 and 5 Collection products. Using 1 km spatial resolution SPOT-VEGETATION data for 11 successive years (2000-2010) and the GlobeCover classification chain, Bontemps et al. (2011b) generated yearly global land cover products and comparison among the products showed that only 41 % of the world was consistently mapped for the eleven successive years. Also, according to the validation report of the GlobeCover 2009 project (Bontemps et al., 2010), up to 50% of some classes were inconsistently mapped between GlobeCover 2005 and GlobeCover 2009 (Figure 1). These differences in land cover label cannot be wholly attributed to changes in the land cover as the annual rate of land cover change at the global scale is less than 1% (Bontemps et al., 2011b). Nevertheless, the temporal inconsistency in land cover label has been found to be more pronounced in areas such as the savannah ecosystem that are highly heterogeneous, have considerable year-to-year variability in phenology, and are consistently under anthropogenic or natural perturbation (Friedl et al., 2010;Hüttich et al., 2011). Reducing these kinds of uncertainties in global land cover products should top the research agenda of the land cover mapping community.

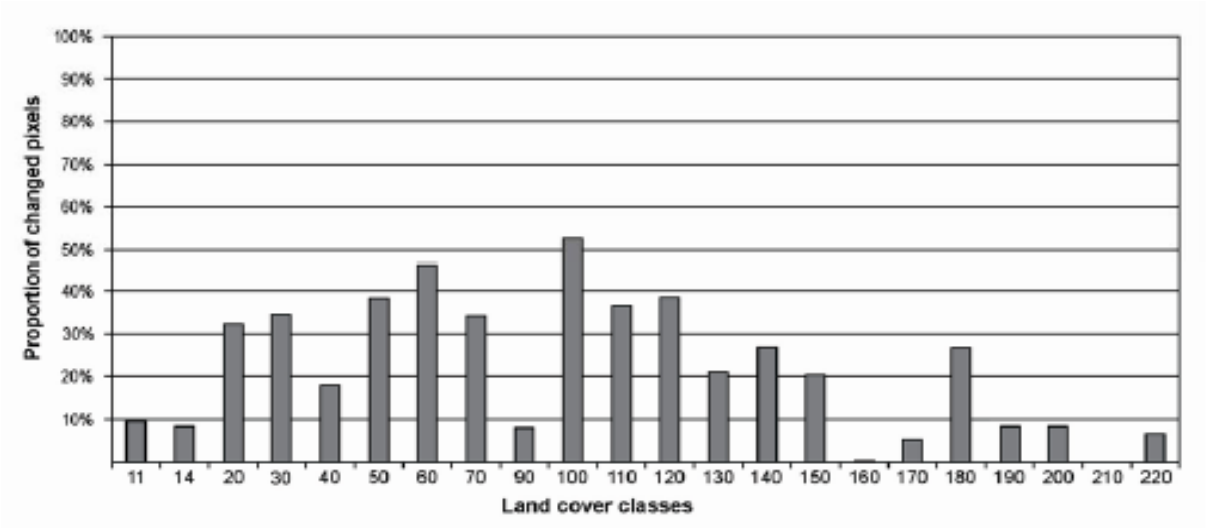

Figure 1: Proportion of pixels, for each class, which are not classified in the same manner between GlobeCover 2005 and 2009. The numbers in for the land cover classes are the original class code for the GlobeCover products (Source: Bontemps et al., 2010).

Changes in observed land cover over time may either be due to changes in the 'land cover state' and/or changes in the 'land cover condition' (Defourny et al., 2011). The land cover state is referred to as the component of the land cover 'which remain stable overtime and thus define the land cover independently of any sources of temporary or natural variability' (Defourny et al., 2011). For example, a boreal forest covered by snow in the winter months should not be classified as permanent snow; a cropland in the off-season might appear as bare soil but it should be classified as cropland and not bare soil. Land cover condition, on the other hand, is the dynamic component of the land cover that 'is directly related to this temporary or natural variability that can induce some variations in land surface features over time but without changing the land cover state in its essence' (Defourny et al., 2011). For example, the land cover condition of a savannah may change several times a year, such as almost barren in the dry season (due to fire or grazing) to full bloom of photosynthetic active vegetation in the rainy season. In asking for a stable land cover map, the CMC demands that land cover maps should faithfully mirror the actual land cover state and not the land cover condition. Unfortunately, the available global land cover products were generated from relatively few instantaneous observations (usually from a single year data) of the land cover state, thus making the classified land cover maps sensitive to the observation period and may reflect temporal conditions (Defourny et al., 2011). There is need to evolve mapping approaches that are less sensitive to the intra— and inter— annual variation in the land cover condition, while making distinction between actual land cover change (change in land cover state) and temporal and/or natural variability. Thus, the current approach of using "single-year" data to produce global land cover products is insufficient in characterizing highly variable systems. Sensitivity of land cover products to inter-annual variation in the 'condition' of the land cover can be overcome through the use of multi-year time series of satellite data. The assumption is that the land cover will be mapped in a consistent manner over time if no land cover change has occurred (Defourny et al., 2011). However, this new approach of using multi-year satellite dataset for land cover classification has not yet been widely investigated within the framework of large-area and global land cover mapping.

While the use of multi-year time series datasets may reduce the sensitivity of the land cover classification output to inter annual variation in the land cover condition, the result of such classification may be misleading when there is a land cover change, defined as 'a permanent modification of the land cover state— and not of the land cover conditions— in comparison with a baseline status' (Defourney et al., 2011). Thus, the proposed approach of using multi-year data to produce stable land cover maps can only be achieved by integrating in the classification chain a robust technique that can identify pixels that have changed and, if possible, differentiate land cover change (or land cover conversion) from natural and/or temporal variability. This proposed approach is a new line of research that needs to be vigorously investigated for large area (regional, global) land cover mapping.

Classification accuracy of land cover products also featured prominently among the requirements of the CMC. Whereas the CMC is desiring a minimum individual class- and overall- accuracy of 85 % (Bontemps et al., 2011b), the overall accuracy of the available global land cover products (Defourny et al., 2009;Friedl et al., 2002;Friedl et al., 2010;Hansen et al., 2000;Loveland et al., 2000) is between 68-73 % (Bontemps et al., 2011b). Classification accuracy of remote sensing imagery is affected by many factors one of which is the quality of the dataset. Clouds, aerosols, snow cover, differing sun zenith angles, and instrumental problems could degrade data quality (Verger et al., 2011). To mitigate this problem, compositing observations at specified time steps are often employed. The currently available global land cover products were generated from composite datasets. Compositing ensures only high-quality observations are used in the classification process and that noise in the data set is removed, thus improving the accuracy of the classification result (Hüttich et al., 2011;Maxwell et al., 2002). However, a recent study by Huttich et al. (2011) has demonstrated that increasing the length of the overall observation period (multi-year) in addition to using compositing technique improves classification accuracy compared to using a shorter observation period (single-year). This investigation was carried out using 250 m resolution MODIS data acquired over the highly variable Kalahari savannah region of Namibia. The findings from this study, particularly the use of longer observation time period, need to be investigated in other ecological and climatic regions of the world.

In response to the needs of the climate modelling community, the ESA CCI Land Cover (LC) project, led by a consortium of scientific and technical experts, recently initiated the *Round-Robin* (RRob) *Activity* in which land cover research scientists can propose and develop approaches to mapping of land cover. The proposed approaches should meet the CMC requirements in terms of accuracy, temporal stability and consistency of the characterized land cover (Herold et al., 2011).

1.3 Research focus, objectives and research questions

In this study, we propose a land cover classification approach that combines multi-year satellite data and stability test to reduce the sensitivity of the classification output to variation in land cover condition. Stability test, also referred to as structural change test, has been proposed in the statistics and econometric literature for testing the stability of linear regression models of time series (Kuan and

Hornik, 1995;Zeileis et al., 2002), for example in analysing exchange rates dynamics (Zeileis et al., 2010). Concepts from stability test have been applied by some investigators in the remote sensing domain to detect drought occurrence in near real-time (Verbesselt et al., 2012), historical changes in the phenological and trend component of remote sensing data (Verbesselt et al., 2010a;Verbesselt et al., 2010b), and monitoring long term greening and browning trend over the entire globe (de Jong et al., 2012). Here we focused on applying the stability test on satellite time series to separate 'stable' pixels from 'unstable' ones prior to land cover classification. While data for the entire observation period for the stable pixels was used as input for land cover classification, only data of the latest year for the unstable pixel was fed into the classification chain. The assumption is that the data of the stable pixels contains no significant land cover change (change in land cover state) as opposed to that of the unstable pixels.

The overriding objective of this study was to use multi-year satellite data and stability test to produce a stable 'best' land cover map (hereafter referred to as STBM) that will be less sensitive to variation in the land cover condition. The specific objectives were to assess the overall- and individual class accuracies of the STBM, and to evaluate how well the approach of using the stability test concept and multi-year satellite data has ensured STBM label stability. For the second specific objective, we narrowed the analysis of label stability to the forest class. Tree-based classes such as forest are considered among the most important land cover classes by a broader group of CMC (Herold et al., 2011). From an ecological and climate change point of view, forest ecosystems, especially the tropical ones, are critical to biodiversity maintenance (Walker, 2012) and to the global carbon cycle.

The following research questions were addressed in order to meet the objectives of this study:

a) Can the use of multi-year satellite data and stability test produce a STBM with satisfactory overall- and individual class accuracies?
b) To what extent are the class labels produced by the approach in the first research question stable over time and unaffected by changes in the land cover condition?

We tested our approach by applying the stability test on the Enhanced Vegetation Index (EVI) (Huete et al., 2002), employed as a proxy indicator of the land cover condition and state. We used MODIS EVI 16-day image composites from 2005 to 2009 acquired over a site encompassing almost the entire State of Mato Grosso in Brazil and extending marginally into Eastern Bolivia. Land cover classification was done using the reflectance and EVI bands of the same MODIS data.

2 Materials and methods

In this section we give a brief description of the study area (2.1) and detail explanations of the data and methods used to achieve the objectives of the study (2.2 – 2.4). Figure 2 gives an overview of the processing sequence and methods that was used in this study.

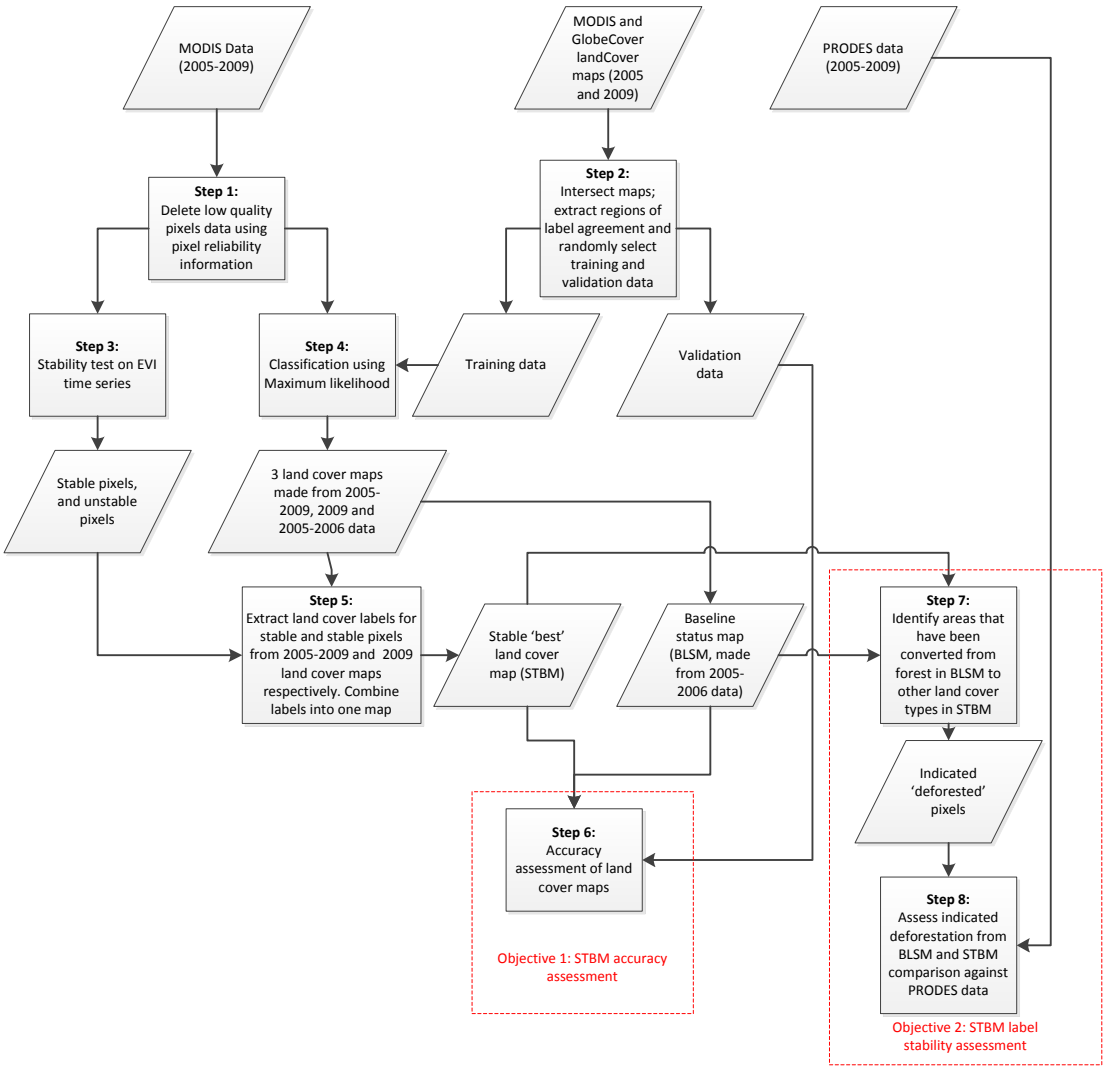

Figure 2: An overview of data, methods and procedures used in this study.

2.1 Study area

The study area extends between latitudes 10°S and 18°S and longitudes 52°W and 58°W, encompassing almost the entire State of Mato Grosso in Brazil and extending marginally into Eastern Bolivia (Figure 3). The extent of the study site is about 679, 708 km^2. The climate is tropical, characterized by a rainy season that lasts from September to April, with an average annual rainfall ranging from 1200 to 2000 mm (Arvor et al., 2012). The landscape is generally undulating (RADAMBRASIL, 1978), with rich diversity of natural vegetation characterized into three major ecoregions: the Amazonian forest, the Cerrado and the Pantanal. These ecoregions are globally acclaimed as hotspots of biodiversity richness (Arvor et al., 2012). Generally, the Brazilian portion of this study site is currently under heavy anthropogenic disturbance, particularly from deforestation

(INPE, 2009;Lima et al., 2012), with cattle ranching and agricultural expansion as major drivers (Arvor et al., 2012;Morton et al., 2006). Soybean is the major (commercial) agricultural crop grown in this region, followed by sorghum or millet (Arvor et al., 2012). Soybean is planted at the onset of the rainy season, usually from late September to early November, and harvested from January to March. Sorghum and millet are usually sowed following the soybean harvest, thus serving as off-season crops.

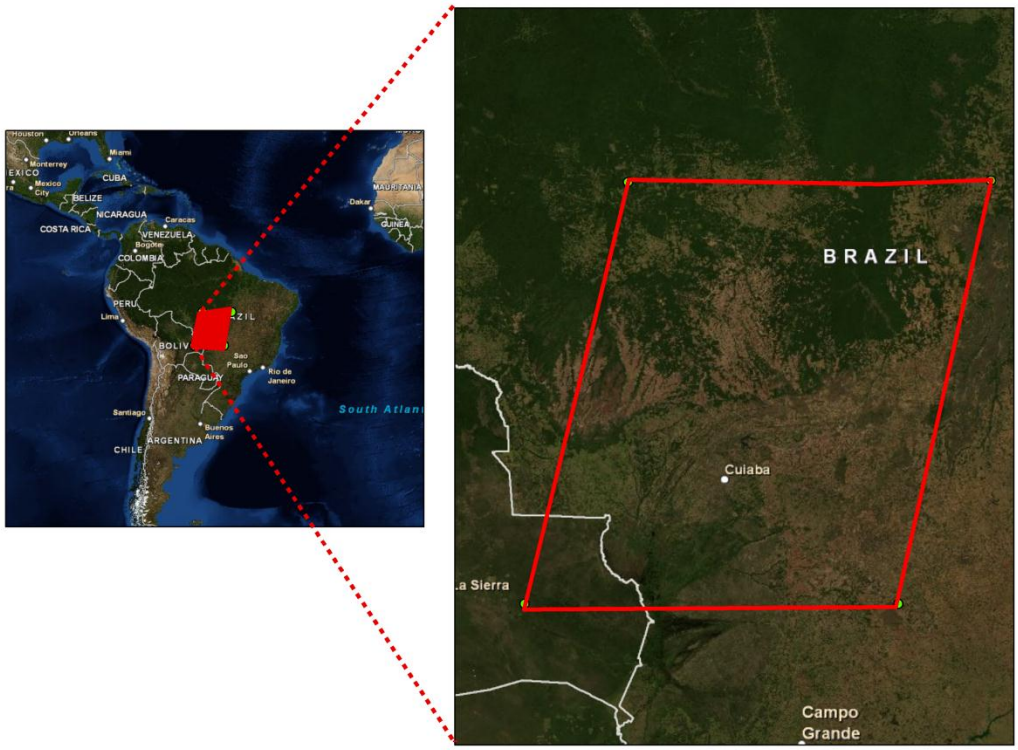

Figure 3: Study area (bounded by red box).

2.2 Data and pre-processing

2.2.1 Satellite data

Time series of MODIS collection 5 product (MOD13Q1, 16-day composites in sinusoidal projection) at the original 232 m resolution and spanning the period from 2005 to 2009 were used as input for both the land cover classification and the label stability analysis. The MODIS Tile h10v12 that covers the study area was downloaded from NASA LP DAAC website (http://reverb.echo.nasa.gov/reverb, last accessed 4 February 2012). Pre-processing included spatial and spectral subsetting to the extent of the study area and of the reflectance and EVI bands, respectively, using the MODIS Reprojection Tool (https://lpdaac.usgs.gov/tools/modis_reprojection_tool/, last accessed 4 February 2012). Because of cloud contamination effects and differing sun zenith angles, low quality data were identified and set to no-data value based on information from the pixel reliability layer. Pixel reliability information ranks

data as: 0 (Good data) 1 (Marginal data) 2 (Snow/Ice) and 3 (Cloudy) (https://lpdaac.usgs.gov/content/view/full/6652, last accessed 4 February 2012). Only pixel data with reliability value of 0 and 1 were retained, as these were least affected by cloud. After 'cleaning', it was observed that poor quality data were concentrated more or less between the months of October to March (1-6 and 18-23 composite days), corresponding to the rainy season in the region (Arvor et al., 2012). Given the poor quality data during the rainy season, only observations from April to September (7-17 composite days), corresponding to time of the year least affected by cloud, were retained and used for classification. However, pixels with less than 80 % of data between this period (April to September) were not classified. For the stability test, the entire time series was used but pixels with more than 40 % of missing or poor quality data were omitted from the analysis. We find 40 % threshold for missing data optimum for this study area as values below this threshold excluded a lot of pixels. We used the entire time series for the stability test because the algorithm can, to some certain extent, cope with missing data (briefly discussed in subsection 2.3.1).

2.2.2 Training and validation data

MODIS International Geosphere-Biosphere Programme (IGBP, 500 m resolution) and GlobeCover (300 m resolution) global land cover maps for the year 2005 and 2009 were adopted as primary sources for training and validation points for the classification scheme, since time, administrative rights and resource constraints made it impossible to obtain field data or fine resolution land cover maps for the study area. The MODIS IGBP is a layer in the MODIS MCD12Q1 collection 5 product which is available online at the NASA LP DAAC website (see subsection 2.2.1). The MODIS Land Cover Product has been produced for each year since 2001, delivering global land cover in five different classification systems including the IGPB. GlobeCover maps (version 2.2 and 2.3) were downloaded from the European Space Agency GLOBCOVER project (http://ionia1.esrin.esa.int/, last accessed 25 September 2011).

The analysis to help answer the second research question was restricted to the forest class and in areas covered by the annual deforestation maps of the Brazilian Legal Amazon (Legal Amazon encompasses the Brazilian territory in the Amazon Basin) produced by the INPE (Instituto Nacional de Pesquisas Espaciais; or National Institute for Space Research), Brazil. We obtained the annual deforestation maps— hereafter referred to as PRODES (Programa de Cálculo do Desflorestamento da Amazônia; or Program for the Estimation of Deforestation in the Brazilian Amazon) data— for the year 2005 to 2009 from a third party: Instituto do Homem e Meio Ambiente da Amazonia (IMAZON), Brazil. PRODES is available online from INPE's digital website (http://www.obt.inpe.br/prodes/, last accessed 25 September 2011). The PRODES maps have been produced on a yearly basis since 1997 (Câmara et al., 2006;Shimabukuro et al., 1998) based on Landsat data. Part of INPE's strategy is to acquire Landsat images around first of August every year, and the images are pre-processed and classified into four classes: water, forest, non-forest and deforestation. See Câmara et al. (2006) for a detailed description of the method used to produce the PRODES maps. The PRODES maps used in this study have been resampled from their original 60 m resolution to a 100 m resolution by IMAZON.

2.3 Stability test methodology

We employed methods for testing structural change in linear regression models of time series proposed in the statistics and econometrics literature (e.g. Zeileis et al., 2002) to analyze the stability of the land cover in our study site over the five years period (2005 to 2009). We used the EVI as a proxy indicator of the state and condition of the land cover. Unlike NDVI (Normalized Difference Vegetation Index) which is sensitive to high biomass region such as evergreen forest (Huete et al., 2002;Verbesselt et al., 2010b), EVI is a good indicator of the land cover dynamics and disturbances for high biomass region such as the site in this study. Before applying the stability test, we preprocessed the EVI time series for subsequent regression modeling using the Time Series Preprocessing for BFAST-Type Models (bfastpp) method documented in the Break for Additive Seasonal and Trend (BFAST) package for R (Development Core Team, 2012, http://cran.r-project.org/package=bfast). The method forms a data frame of the observed data (in this case EVI) consisting of a response term, seasonal terms, a trend term, (seasonal) autoregressive terms, and covariates. A model based on one or more of the terms can be fitted to the observed time series data.

2.3.1 Harmonic-seasonal model

Several models such as the trend-seasonal model (Verbesselt et al., 2012), the harmonic-seasonal model (Verbesselt et al., 2010b); or a constant term (intercept)-based model (e.g. Zeileis et al., 2002) can be fitted to the time series of the observed data and subsequent analysis using techniques from structural change literature can be used to test for the stability of the observation. But in this study, we opted for the harmonic-seasonal model as preliminary stability test (not detailed here) performed on some subsets of our study area showed the stability test agreeing more with PRODES data for unstable areas (deforestation in this case) when this model was used compared to the other two models. Figure 4 depicts an example of fitting linear regression models to a time series data using harmonic-seasonal-, trend-seasonal- and a constant (intercept) model.

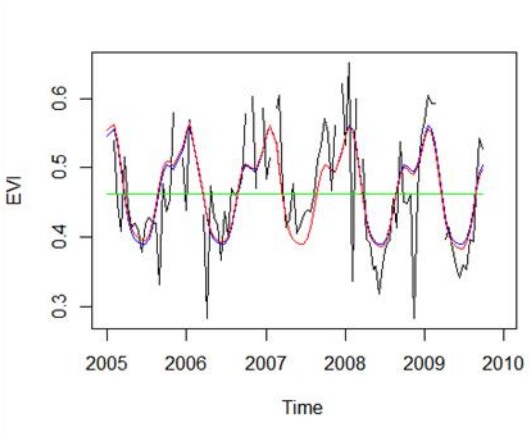

Figure 4: Harmonic-seasonal model (in red), trend-seasonal model (in blue) and constant term (in green) model fitted to an EVI time series (in black) of a pixel in the study area using ordinary least square (OLS) method. Only the first three harmonic components were used to fit the harmonic-seasonal and the trend-seasonal models.

Following (Verbesselt et al., 2010b), the harmonic-seasonal model (S_t) can be written in the form:

$$S_t = \sum_{k=l}^{k} a_{j,k} \; sin\left(\frac{2\pi kt}{f} + \delta_{j,k}\right) \qquad (1)$$

where the amplitude $a_{j,k}$ and phases $\delta_{j,k}$ are the unknown parameters and f is the known frequency (e.g., f = 23 annual observations for a 16-day time series). The model (Eq. 1) can be conveniently transformed to a multiple linear harmonic regression model as (Verbesselt et al., 2010b):

$$S_t = \sum_{k=l}^{k} \left[\gamma_{j,k} \; sin\left(\frac{2\pi kt}{f}\right) + \theta_{j,k} \; cos\left(\frac{2\pi kt}{f}\right)\right] \qquad (2)$$

where the coefficients $\gamma_{j,k} = a_{j,k}\cos(\delta_{j,k})$ and $\theta_{j,k} = a_{j,k}\ \sin(\delta_{j,k})$ can be easily estimated. The model can also be written as a standard linear regression model (adapted from Verbesselt et al., 2012):

$$y_t = x_t{}^T \beta_t + \varepsilon_t \qquad (3)$$
$$x_t = [sin(2\pi 1t/f),\ cos(2\pi 1t/f), \ldots sin(2\pi kt/f), cos(2\pi kt/f)]^T,$$
$$\beta = [\gamma_1 cos(\delta_1), \gamma_1 sin(\delta_1), \ldots\ldots \gamma_k cos(\delta_k), \gamma_k sin(\delta_k)]^T,$$

where at time *t,* y_t is the observation of the dependent variable, x_t is a vector of regressors, ε_t is the unobservable error term with standard deviation σ and β_t is the k-dimensional vector of regression coefficients. The regression parameter β can be estimated and tested using ordinary least square (OLS) techniques (Verbesselt et al., 2012). When there are gaps in the time series,y_t the observations are omitted prior to the estimation of β which can still be identified in a consistent manner (provided there are still some observations at certain frequencies) (Verbesselt et al., 2012). However, prior to the structural change test we had excluded pixels with more than 40% missing data.

Some of the advantages of harmonic-seasonal model (Eq.1) are: it less sensitive to short-term data variations and inherent noise (e.g. clouds), and it is relatively fast as fewer observations are required because only few parameters (a_j, δ_j) are estimated in the multiple regression model (Verbesselt et al., 2010b). Harmonic analysis has been used to study inter annual variations in plant growth cycle (Geerken, 2009;Ronald Eastman et al., 2009;Wagenseil and Samimi, 2006); to characterize annual growth cycle for the purpose of land cover classification (Geerken, 2009;Wagenseil and Samimi, 2006); and for phenological change detection (Verbesselt et al., 2010b).

2.3.2 Structural change:

In structural change theory (e.g. the work of Zeileis et al., 2002), the null hypothesis of 'no structural change' in the observed data assumes that the regression coefficients β are constant over time:

$$H_0: \ \beta_t = \beta_o \qquad (t=1 \ldots n) \qquad (4)$$

However, when there is some change(s) in the observed data, the OLS estimate of regression coefficient $\hat{\beta}$ based on observations at some specified period of time within the observation period will

be different from the OLS estimate of the regression coefficient $\hat{\beta}$ based on all observations over the entire observation period. In simple terms, if there is a structural change in the data, the OLS estimate of the regression coefficients based on the entire data should be appreciably different from the OLS of the regression coefficients estimate based on subsamples of the data that are without structural change(s). On the contrary, these estimates should be somewhat similar if the true coefficients are invariant over time. The OLS residuals are denoted by $\hat{\varepsilon}_t = \hat{y}_t - \hat{x}_t^T \hat{\beta}$ with a variance estimate $\sigma^2 = \frac{1}{n-k}\sum_{t=1}^{n} \hat{\varepsilon}_t^2$ (Zeileis et al., 2002).

In this study, we used the ordinary least square (OLS) residuals–based moving sums (OLS- MOSUM) to test whether there is some structural change in the observed data over time. The OLS-MOSUM procedure computes an empirical process from the differences in the OLS residuals between subsamples estimates and the overall observation OLS residual estimate (Zeileis et al., 2002). The subsamples are selected by a window of constant width h (h is chosen relative to the size of the observation period, e.g. h = n/5 or h = n) that moves over the entire sample period. The OLS-MOSUM process is given by (see Zeileis et al., 2002):

$$M_t^o\left(\frac{t}{h}\right) = \frac{1}{\hat{\sigma}\sqrt{n}}\left(\sum_{i=[N_n t]+1}^{[N_n t]+[nh]} \hat{y}_t - \hat{x}_t^T \hat{\beta}\right) \qquad (0 \le t \le 1-h) \qquad (5)$$

where $N_n = ([nh])/(1-h)$.

Under the null hypothesis of 'no structural change', the empirical process ($M_t^o\left(\frac{t}{h}\right)$) should not fluctuate or deviate too much from its mean which is zero. On the contrary, if there is structural change(s), the empirical process show large fluctuation and asymptotically crossed some boundary at certain controlled probability, ∝. Figures 5 shows an example of an OLS-MOSUM test where the computed empirical fluctuation process crossed and did not cross the boundary. The reader is referred to Zeileis et al. (2002) for an in depth explanation on the theoretical underpinnings of the structural change test.

2.3.3 Application of stability test

We applied stability test on the EVI time series after fitting a linear model (using OLS) based on the harmonic-seasonal term. We used the first three harmonic terms (k = 3, equation 2) for our fitting, since the fourth and higher terms characterize variations occurring in cycles equal to or less than three-months (Verbesselt et al., 2010b). We chose a window of size 0.25 (i.e. h = 0.25, equation 5), corresponding to 1.25 years of our observation period, for the OLS-MOSUM process. Our choice of 1.25 years as the window width was not based on any theoretical foundation; however, we chose this value after preliminary stability test (not detailed here) performed on subsets of the study area using window sizes of 2 years (i.e. *h* = 0.4) and 1.25 years showed similar results. We considered a pixel unstable only when the stability test indicates a significant structural change at *p* <0.05.

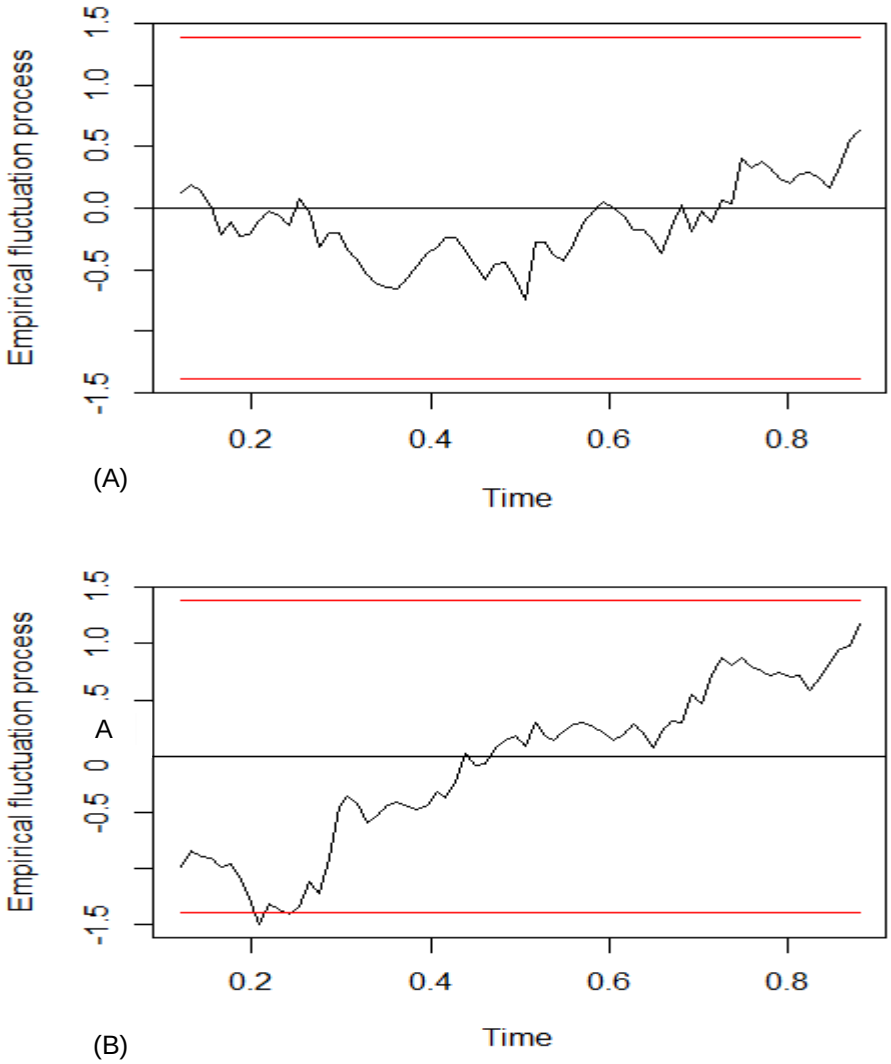

Figure 5: Stability test performed on two pixels (A and B) in our study area. No structural change in pixel A; a significant change ($p < 0.05$) in pixel B as the empirical fluctuation process crossed the boundary.

2.4 Production of stable 'best' land cover map (STBM)

The overriding objective of this study was to produce the STBM. By 'stable' we mean that the land cover map should be insensitive to variation in the land cover condition, meaning that the labels on the maps should closely mirror the true 'state' of the land cover. In addition to the production of the STBM, a second map to act as the baseline status map (hereafter referred to as BLSM) was produced to adequately address the second specific objective (details of the production of BLSM are given in parts of subsection 2.4.2).

Figure 6 gives a general overview of the procedure that was followed to produce a STBM of the study area. The stability test was applied to the EVI time series to distinguish between pixels whose land cover was stable from those that were unstable. We assumed that the instability of land cover was largely due to change in the state of the land cover. Preliminary stability test performed on some subsets (largely forest dominated areas) seems to agree with our assumption as most unstable areas were also recorded as deforested by the PRODES data. Stable and unstable pixels were classified

using the entire time series and the latest satellite data respectively. By using the entire time series to classify stable pixel, we were poised to reduce the sensitivity of the classification process to variability in the land cover condition.

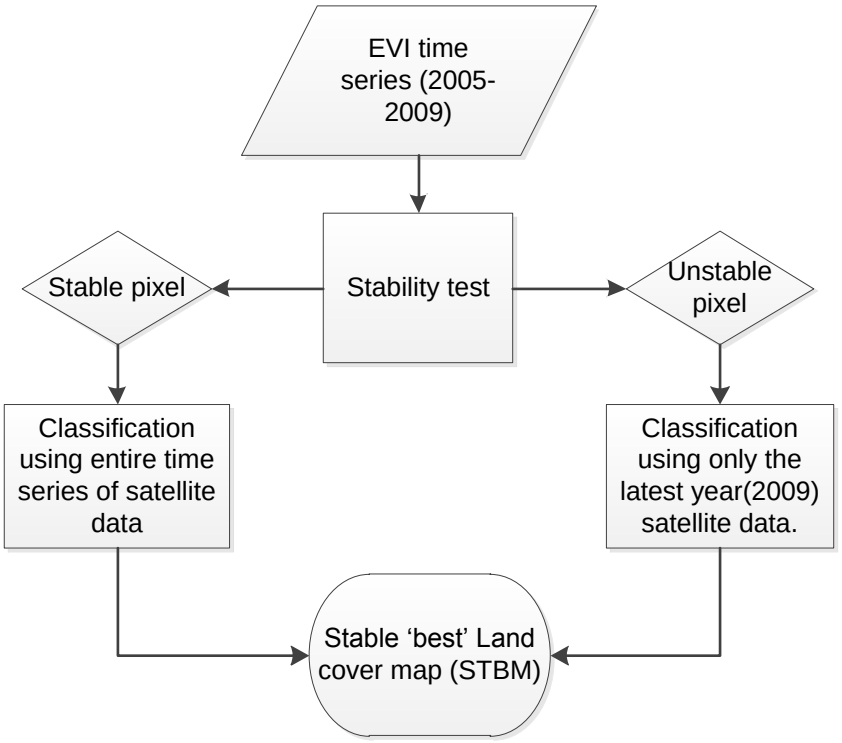

Figure 6: A schematic overview of the use of stability test and multi-year satellite data to produce stable 'best' land cover map (STBM) for the study area.

.

2.4.1 Training and validation scheme

With nominal pixel sizes of 300 m and 500 m, respectively, GlobeCover and MODIS (Collection 5 products) represent the highest spatial resolution land cover products currently available. However, GlobeCover and MODIS IGBP maps are by no means free from errors (Bontemps et al., 2011a;Friedl et al., 2010), particularly as any map is more or less a model or generalization (Foody, 2002). Like we highlighted earlier, the available global land cover products were made from single year data, thus making them sensitive to variation in land cover condition. However, to minimise the chances of propagating the errors in these maps to our thematic map, we selected only points with label agreement between both maps to form our training and validation datasets. To achieve this, we first aggregated the legends of each of the maps and subsequently harmonized them into five classes, namely: *Forest, Croplands and cropland/vegetation mosaics*, *Other vegetation and mosaics*, *Urban and barren*, and *Water* (Table 1). The GlobeCover map was reprojected to the same reference system (Sinusoidal) as the MODIS IGPB and the MODIS image to be classified. Second, we made subsets of the reference maps to the extent of the study area. Third, the reference maps were vectorized and intersected in ArcGIS 10.0. Polygons with label agreement between the land cover reference maps (Figure 7) based on the five new classes (Table 1) were extracted to form a new dataset. The new dataset was intersected with a grid of 500 m by 500 m, corresponding to four MODIS pixels of our

image, to avoid sampling large polygon (or number of pixels), since neighbouring points (or pixels) are not completely independent of each other and could be redundant in a cluster of pixels (Congalton and Green, 1999). However, polygons that are less than one MODIS image pixels size (62, 500 m^2) were excluded from the newly created datasets.

Table 1: Aggregated and harmonized legends of GlobeCover and MODIS IGPB

New legend	GLOBCOVER	MODIS IGBP
Forest	Closed to open broadleaved evergreen or semi-deciduous forest [40][a]	Evergreen needleleaved forest [1]
	Closed broadleaved deciduous forest [50]	Deciduous needleleaved forest [3]
	Open broadleaved deciduous forest [60]	Evergreen broadleaved forest [2]
	Closed needleleaved evergreen forest [70]	Deciduous broadleaved forest [4]
	Open needleleaved deciduous or evergreen forest [90]	Mixed forests [5]
	Closed to open mixed broadleaved and needleleaved forest [100]	
	Closed to open broadleaved forest regularly flooded (fresh-brackish water) [160]	
	170 - Closed broadleaved forest permanently flooded (saline-brackish water)	
Urban and barren	Sparse vegetation [150]	Urban and built-up land [13]
	Artificial areas [190]	Barren or sparsely vegetated [16]
	Bare areas [200]	Permanent snow and ice [15]
	Permanent snow and ice [220]	
Water	Water bodies [210]	Water [0]
Other vegetation and mosaics	Closed to open shrubland [130]	Woody savannahs [8]
	Closed to open grassland [140]	Savannahs [9]
	Mosaic Forest-Shrubland/Grassland [110]	Grasslands [10]
	Mosaic Grassland/Forest-Shrubland [120]	Closed shrublands [6]
	Closed to open vegetation regularly flooded[180]	Open shrublands [7]
		Permanent wetland [11]
Croplands & croplands/vegetation Mosaics	Irrigated croplands [11]	Croplands[12]
	Rainfed croplands [14]	Cropland/natural vegetation Mosaics [14]
	Mosaic Croplands/Vegetation [20]	
	Mosaic Vegetation/Croplands [30]	

[a] Numbers in brackets refer to the original class codes for the individual datasets.

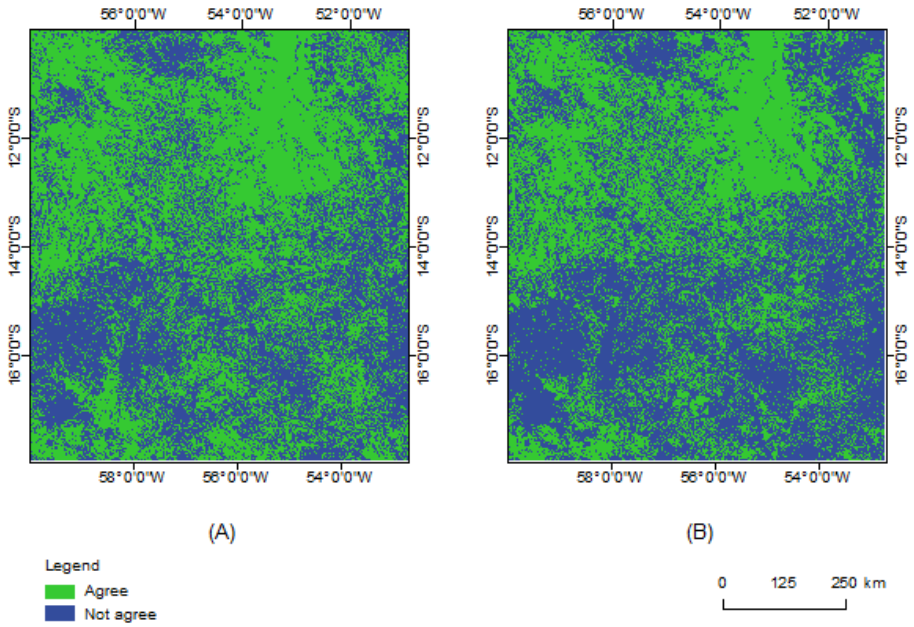

Figure 7: Areas of label agreement and disagreement between aggregated and harmonized legends of GlobeCover and MODIS IGPB land cover maps for the study area in year 2005 (A) and year 2009 (B). There are more areas of label agreement between the land cover product in 2005 (54.5 % of the study area) than in 2009 (45.8 % of the study area).

A random sampling approach was used to select the training and validation points on a per class basis. Briefly, each of the five classes was separately extracted from the dataset created as described in the preceding paragraph. From each of the class dataset, except for the *Urban and barren* class, about 2,200 to 2,500 polygons were randomly selected using the Random tool in Quantum GIS to form the reference data for that class. Thirty per cent (30%) of the reference data was randomly selected and kept for validation, while the remaining 70 % was kept for training; this guarantees that no point or set of points will be used for both training and validation, thus removing any bias.

Table 2 shows the number of polygon features of the training and validation samples and the total number of image pixels contained in the polygons after rasterization. Number of training and validation pixels was fewer for the urban and barren class as this class covered a smaller area of the landscape. More pixels were sampled for the water class because preliminary analysis (not discussed here) showed that pixels with more data gaps in the time series are located within the water areas. And in this study, pixels with less than 80 % observations (base on composite days 7-17) were not classified.

Table 2: Number of Training and validation polygons and pixels randomly picked (per class bases) from areas of label agreement between GlobeCover and MODIS IGPB global land cover maps for the year 2005 and 2009

Year	Class	Training		Validation	
		Number of Polygons	Number of pixels	Number of Polygons	Number of pixels
2005	Forest	1508	5909	651	2,595
	[a]CCVM	1488	4214	640	1,742
	[b]OVM	1484	4426	640	1,994
	Urban and barren	134	494	55	190
	Water	1719	6922	740	2,937
2009	Forest	1511	5,870	644	2,497
	CCVM	1486	4,491	631	1,975
	OVM	1476	4,304	645	1,894
	Urban and barren	134	467	59	185
	Water	1725	6,877	741	3,010

[a] CCVM= Cropland and cropland/vegetation mosaics
[b] OVM =Other vegetation and mosaics

2.4.2 Classification

Maximum likelihood classifier (MLC) was adopted as the algorithm for classification in this study. MLC, a probalistic classifier, is one of the widely used classification algorithms for remote sensing data to produce both hard and soft outputs (Xu et al., 2005). One of the advantages of MLC is that, unlike most supervised classifiers such as the minimum distance classifier, it models well asymmetrical class distributions elongated at different degree and directions in multispectral space. Thus, applied correctly, MLC will reduce average classification error to a minimum (Richards and Jia, 2006). However, one major disadvantage with the MLC is the assumption that the data is normally distributed, an assumption which may not always hold true with remote sensing data.

Composite images of the blue (459-479 nm), red (620-670 nm), near infrared (NIR, 841-876 nm), middle infrared (MIR, 1230-1250 nm) and EVI of the MODIS data were used as the input features for the classification process. Classification was done in the Environment for Visualizing Images— ENVI— 4.8 software (ENVI; Research Systems, Boulder, CO). The BLSM was classified using satellite data of 2005 and 2006. We used two years data as against one year data to classify the BLSM so as to increase the chances of mapping the actual land cover state. This was necessary for our study site especially as there was prevalence of drought over a larger portion of the Amazon in 2005 and this drought provoked extensive fire events that penetrated dense forest stands (Brown et al., 2006). However, it was the training data collected for 2005 that was used for the classification of the BLSM.

Two intermediate maps were classified prior to the generation of the STBM. One of the maps was classified using data from the entire time series (2005-2009) and the other using data for 2009 only. These maps were classified with training points collected for year 2009 (Table 2). After the stability

test, class labels of the unstable pixels in the map made with the entire time series data were replaced with labels from the land cover map made from the 2009 data to produce the STBM. This operation was carried out in ArcGIS 10.0. Table 3 shows the number of input features that were used for the classification process of the land cover maps. Only data for composite days 7-17 were used for classification as the other composite days (1-6 and 18-23) were more affected by cloud cover as detailed before.

Table 3: Number of input features used for the land cover classification

Land cover map	Number of input features
2005-2006 land cover	110 (5*22 composite days)
2009 land cover	55 (5*11 composite days)
2005-2009 land cover map	275 (5*55 composite days)

2.4.3 Accuracy assessment of classified maps

Validation of the STBM and BLSM was performed using validation data for 2009 and 2005 respectively. Since the stability test excludes pixels with more than 40% of missing data, validation points that fall on the excluded pixels were removed prior to the validation of the STBM. The percentage of the original validation points (Table 2, data for 2009) that were excluded are 23, 18, 0.48 and 0.15 for the *water*, *Urban and barren*, *Other vegetation and mosaics*, and *Croplands and croplands/vegetation mosaics* classes respectively. Confusion matrix was computed as part of the validation scheme and the overall, user's and producer's accuracies were extracted from the results.

2.4.4 Assessment of land cover stability of STBM

Figure 8 depicts the procedure we adopted to evaluate the stability of the STBM. We assumed that the difference between the STBM and BLSM should only be due to change in the state of the land cover. We focused only on the forest change (deforestation) between 2006 and 2009, since we only have reference data for deforestation. We estimated forest change by the following procedure detailed in the following steps: First, both maps were vectorized and the forest class was extracted from the BLSM. Second, areas in the STBM corresponding to the extracted forest areas in the BLSM (from step 1) were clipped out. Third, the clipped out feature from the STBM was 'subtracted' from the forest shape file of the BLSM, with the difference representing deforestation over 2006-2009. These operations were performed in ArcGIS 10.0.

Areas indicated to be deforested from 'subtracting' STBM and BLSM were evaluated against PRODES data for 2006-2009. This was to enable us assess if the indicated deforestation agrees with PRODES data or not. The total area indicated as deforested from the STBM and BLSM comparison that agrees with PRODES deforestation data was expressed as a percentage of the total deforestation recorded by PRODES. We went a step further to evaluate areas where STBM and BLSM comparison indicated deforestation but PRODES data did not, and vice versa. This evaluation was performed employing Breaks For Additive Seasonal and Trend (BFAST) method proposed by Verbesselt et al. (2010a and b). We employed BFAST to enable us: first, check whether or not there was change in the areas of

disagreement between PRODES data and the STBM and BLSM comparison; second, see whether the change has led to temporal or permanent modification of the land cover within the observation period. These observations would help us to draw conclusions on whether or not there was deforestation in areas of disagreement. The BFAST method was developed to detect trend and seasonal (phenological) changes in ecosystem using satellite image time series (Figure 9). BFAST combines the decomposition of time series into trend, seasonal, and remainder components with methods for detecting change (Verbesselt et al., 2010a and b). A change in the trend component is often an indication of disturbance such as fire, insect attack and flood, whereas a change in the seasonal component represents phenological change such as in the conversion of one land cover type to another (Verbesselt et al., 2010b). A change can be further characterized by its magnitude and direction, which can be derived from BFAST analysis. For detail explanation of the BFAST algorithm, the reader is referred to Verbesselt et al. (2010a and b).

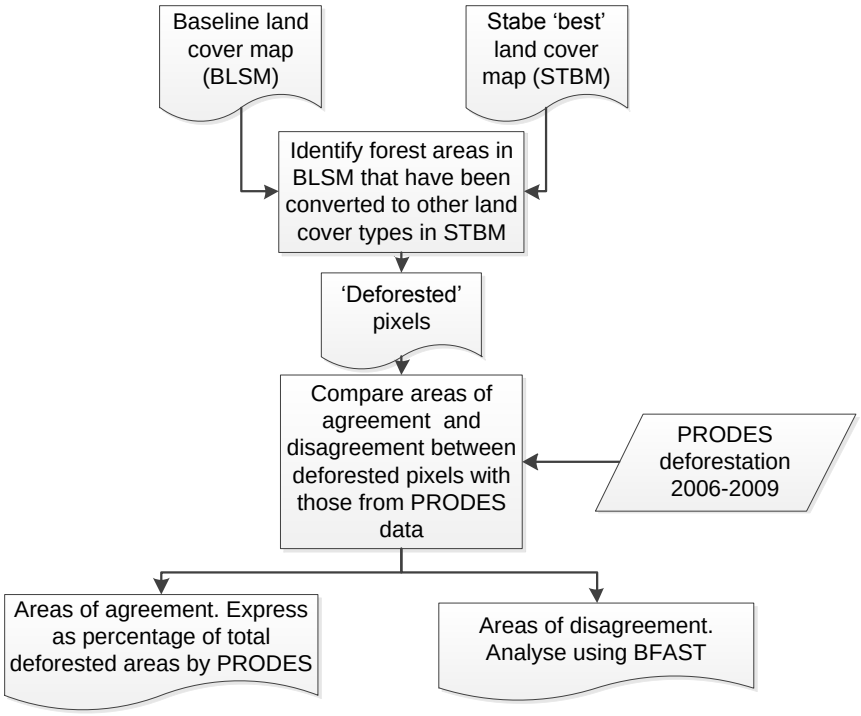

Figure 8: Assessment scheme for land cover stability.

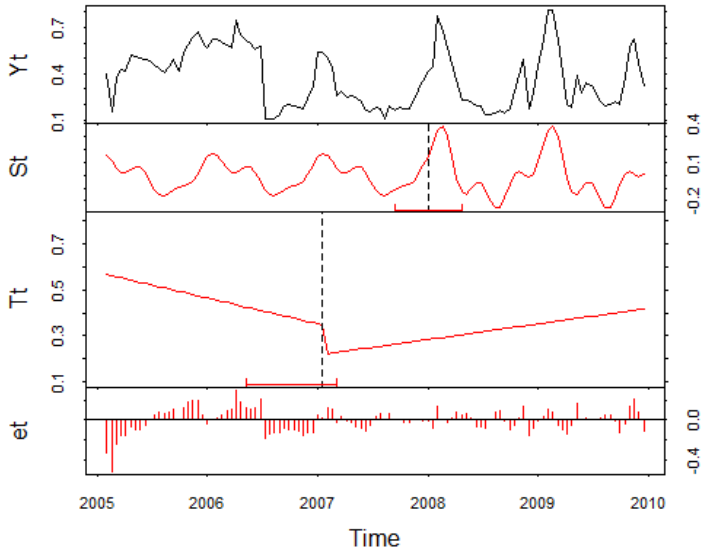

Figure 9: An example of BFAST output obtained by the application of the algorithm on 16-day EVI of a pixel in the study area. The observed data (black) is decomposed into the seasonal, trend and remainder components (red). The seasonal (St) and trend (Tt) component, respectively, contain a phenological and an abrupt change (vertical black dotted lines) with confidence intervals (red).

BFAST analysis was performed on the EVI (2005-2009) of randomly selected pixels in three different cases of disagreement involving PRODES data, BLSM and STBM, and stability test. The first case involved areas where PRODES data showed deforestation and stability test showed structural change (or instability) but BLSM and STBM comparison showed otherwise. A total of 17 pixels were analysed in this case. The second case was similar to the first except that stability test did not show structural change. Fourteen pixels were selected in this case category. In the third case both PRODES and stability test showed no change but BLSM and STBM comparison indicated deforestation. Twenty one pixels were analysed in this case.

For BFAST analysis, the minimum period between breaks was set to two years, meaning that detected change is occurring over a minimum period of two years. Only PRODES deforestation from 2007 and beyond was considered for the analysis because of the two years minimum break period adopted for the BFAST algorithm in this study. Before applying BFAST to the EVI time series, missing values were replaced by linear interpolation between neighbouring values within the time series.

3 Results

3.1 Stability test, classification of stable and unstable pixels

Figure 10 shows the result of the stability test using the OLS-MOSUM process. Overall, about 165, 365.52 km^2 (representing about 24 %) of the 679, 708 km^2 total extent of the study area was unstable over the observation period. The unstable pixels were more or less distributed entirely over the study area, with some large, contiguous clusters localized in certain areas. Most of these large, contiguous clusters of unstable pixels were classified as forest based on 2009 data (Figure 11A). These forests may have been disturbed (e.g. by fire, selective logging, and drought) at the early stages of the observation period but only to recover at the latter stages. Overall, the proportion of the unstable pixels among the land cover classes after classification was in this order: *Other vegetation and mosaics* (45 %) > *Cropland and cropland/vegetation mosaic* (30.6 %) > *Forest* (23.5 %) > *Urban and barren* (0.42 %) > *Water* (0.33%). The distribution of the land cover classes among the stable pixels (Figure 11B) was in this order: *Other vegetation and mosaics* (39.2 %) > *Forest* (31.5 %) > *Cropland and cropland/vegetation mosaic* (28.9 %) > *Water* (0.22%) > *Urban and barren* (0.008 %).

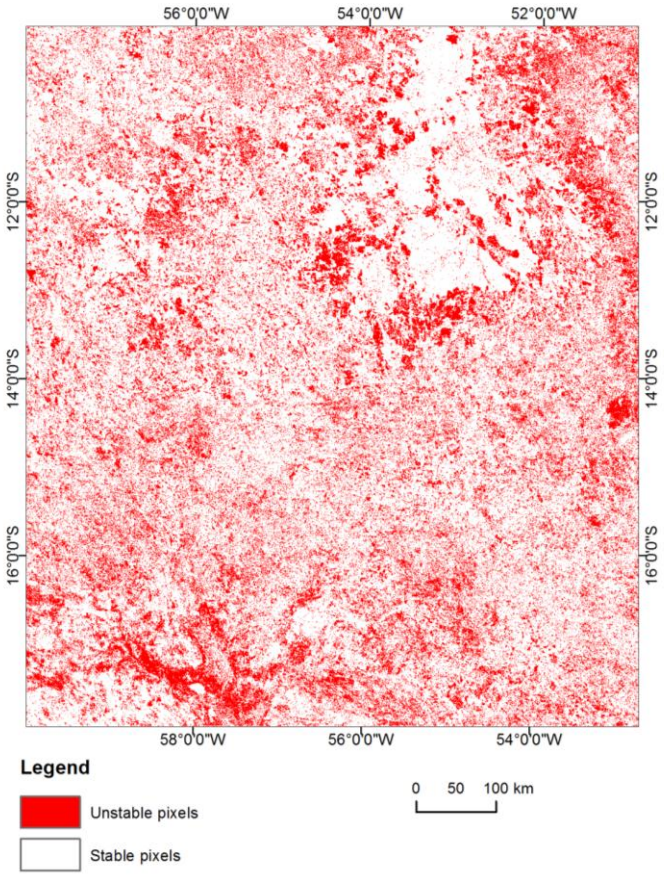

Figure 10: Distribution of stable and unstable pixels in the study area after stability test was performed on the EVI time series.

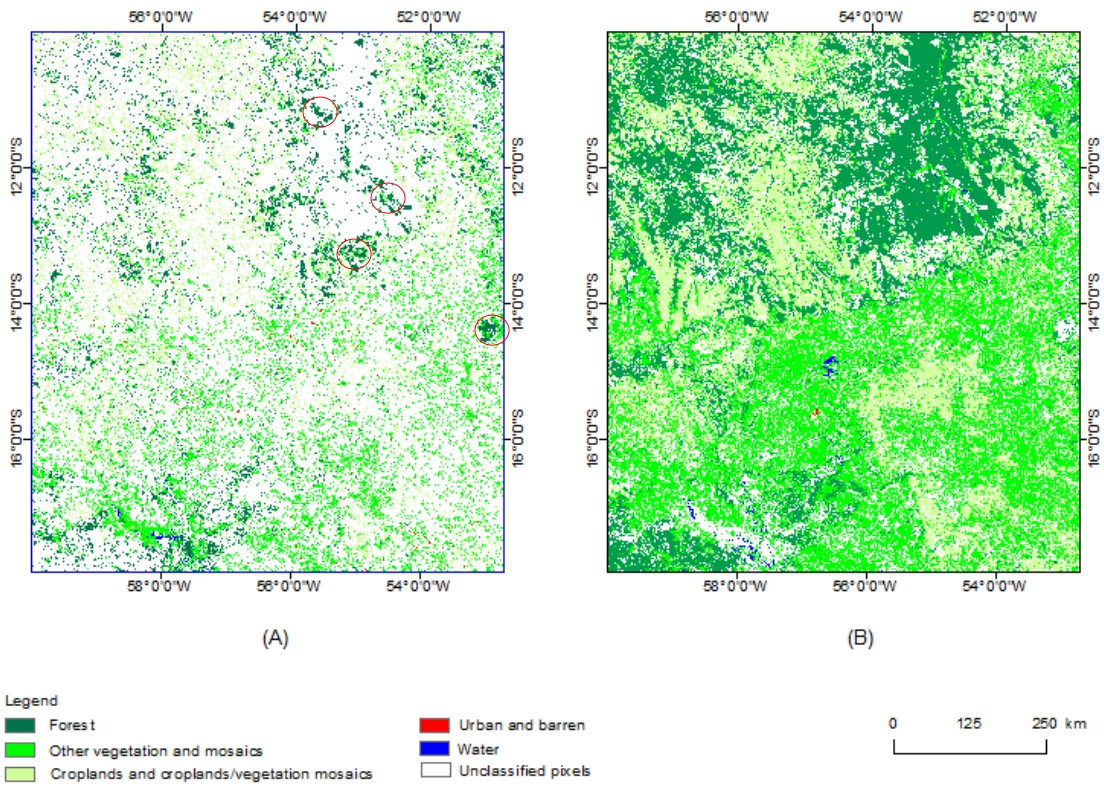

Figure 11: Land cover of unstable (A) and stable (B) pixels. Unstable pixels were classified with 2009 data, whereas stable pixels were classified with 2005-2009 data. Quite a number of contiguous cluster of unstable pixels were classified as forest (few examples are encircled in red).

3.2 STBM and BLSM accuracy assessment

Figure 12A and B depict the classified STBM and BLSM respectively. The error matrixes of the maps are presented in Tables 4 and 5 in the same order. The overall accuracies of both maps are high. Also, except for the producer's accuracies of the *Urban and barren* class in the STBM and the *Other vegetation and mosaics* class in the BLSM, the individual class accuracies (user's- and producer's accuracies) are higher than 80 %. The relative low producer's accuracy (60.9 %) of the *Urban and barren* class in the STBM indicates that a large number of areas that actually belong to this class in the real world are omitted from the class. This explains why more pixels were classified as *Urban and barren* in the BLSM than in the STBM

The user's accuracy— defined as the probability that a sample (i.e. pixel) from land cover map actually matches the real world— was consistently higher for the individual classes in the STBM than in BLSM. Based on the user and overall accuracies, the STBM can be considered as little more accurate than the BLSM.

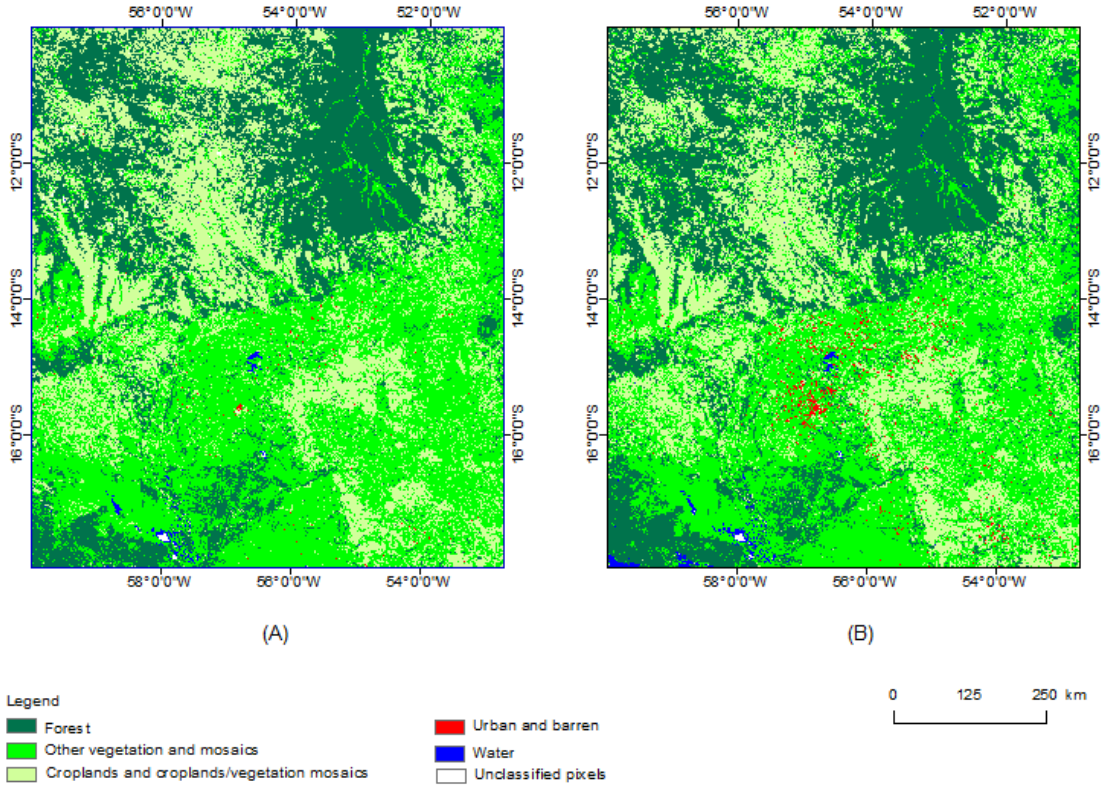

Figure 12: Stable 'best' land cover map (STBM, A) and baseline status map (BLSM, B). One obvious difference between both maps can be seen in the number of pixels classified as *urban and barren* (in red).

Table 4: Error matrix for validation of stable 'best' land cover map (STBM)

Classification	Reference						
	Forest	[a]CCVM	[b]OVM	Urban & barren	Water	Total	User acc.
Forest	2286	9	74	0	0	2369	96.5%
CCVM	82	1864	233	35	0	2214	84.2%
OVM	129	99	1575	22	49	1874	84.0%
Urban &barren	0	0	1	92	0	93	98.9%
Water	0	0	0	2	2075	2077	99.9%
Total	2497	1972	1883	151	2124	8627	
Producer acc.	91.6%	94.5%	83.6%	60.9%	97.7%		91.5%

[a] CCVM= Cropland and cropland/vegetation mosaics
[b] OVM =Other vegetation and mosaics

Table 5: Error matrix from validation for baseline status map (BLSM)

Classification	Reference						
	Forest	[a]CCVM	[b]OVM	Urban & barren	Water	Total	User acc.
Forest	2424	8	148	0	0	2580	94%
CCVM	46	1560	279	24	4	1913	81.6%
OVM	116	169	1536	4	12	1837	83.6%
Urban &barren	0	5	30	162	0	197	82.2%
Water	9	0	1	0	2110	2120	99.5%
Total	2595	1742	1994	190	2126	8647	
Producer acc.	93.4%	89.6%	77.0%	85.3%	99.3%		90.1%

[a] CCVM= Cropland and cropland/vegetation mosaics
[b] OVM =Other vegetation and mosaics

3.3 Assessment of stability of the stable 'best' land cover map

Figure 13A displays the forest areas in the BLSM that have been converted to other land cover types in the STBM. This forest change is in the region covered by the Legal Amazon. The forest change was compared with PRODES deforestation data. Figure 13B depicts deforestation from 2006 to 2009 as recorded by PRODES for this area. About 5, 914.62 km^2 of the area was deforested according to the PRODES data, whereas the deforestation from BLSM and STBM comparison puts this figure around 28,287.40 km^2. Of the 5, 914.62 km^2 deforested area recorded by PRODES, 1,965.87 km^2, representing about 33.2 %, was also captured as deforested by BLSM and STBM comparison. Stability test result when compared to PRODES data showed that only 4,394.1 km^2, representing 76.1 %, of the total area recorded by PRODES data were unstable. The lack of total agreement between PRODES data and BLSM and STBM comparison may be partly attributed to the difference in pixel resolution between the PRODES data and our maps. Land cover changes occurring at scales lower than the coarse resolution of our MODIS image but greater than the Landsat resolution can only be captured by Landsat alone.

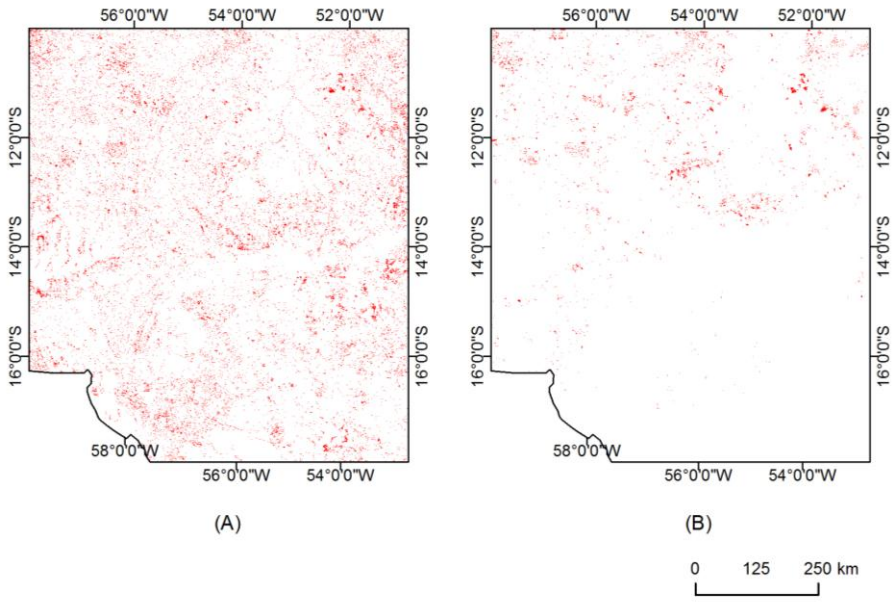

Figure 13: 'Deforested' areas between 2006-2009 (in red) from comparison of STBM and BSLM (A) and as captured by PRODES data (B) for the study area in the Legal Amazon. Deforestation in the portion of the study area in Eastern Bolivia is not shown.

Figure 14 shows BFAST analysis of 4 out of 17 randomly selected pixels in areas where BLSM and STBM comparison did not show any deforestation but PRODES data and the stability test revealed deforestation and instability respectively. Fourteen out of the 17 pixels examined show an abrupt break with a negative magnitude in the trend component and immediately followed by a gradual change with a positive slope, indicating recovery (e.g. Figure 14A). The recovery almost always resulted in the EVI reverting to the initial value, and sometimes even higher than the initial value. This result suggests that the abrupt break may not be due to deforestation but some kind of disturbance

such as forest fire, drought, insect infestations or selective logging. These kinds of disturbances may not necessarily lead to a permanent conversion of the forest cover to some other land cover types, particularly as the forest may have the inherent ability to recover once conditions are favourable. Unfortunately, this result also suggest that PRODES data may sometimes confounds temporal forest disturbance with deforestation and this never gets to be corrected in subsequent annual PRODES data since secondary forest is never considered (Câmara et al., 2006). The consequence is that once an area of land under primary forest is, correctly or incorrectly, captured as deforested, it remains so in the subsequent annual PRODES data even if there was forest regrowth (or reforestation).

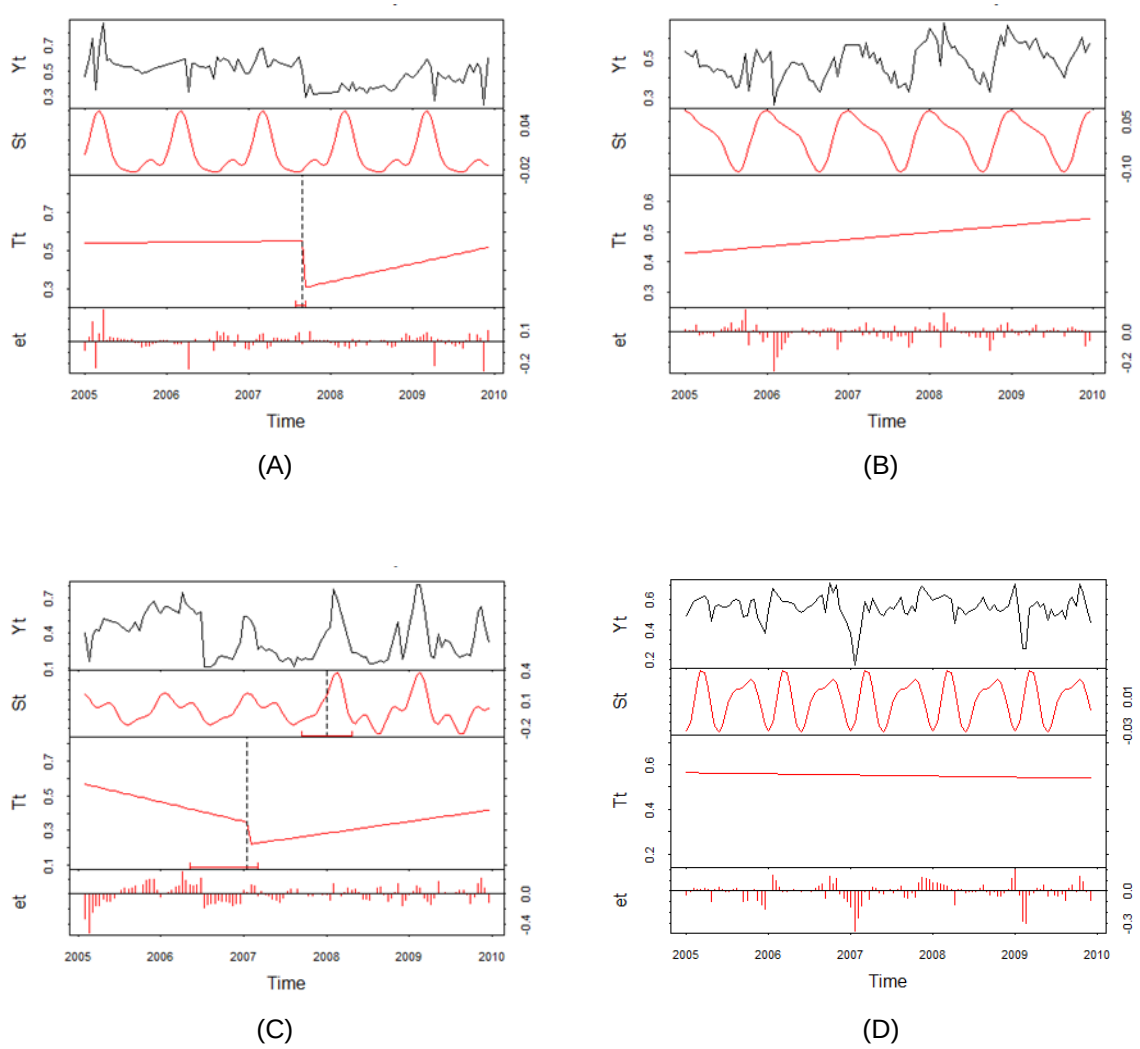

Figure 14: BFAST analysis of some pixels in areas where PRODES data and stability test indicate deforestation and structural change, respectively, but BLSM and STBM comparison showed no change. BFAST results show an abrupt change followed by a gradual change with positive slope (A); a gradual change with positive slope in the trend component (T_t) (B); a phenological change in the seasonal component (S_t) and abrupt change in T_t component(C); and no change (D).

The other 3 pixels that were examined show varying results. One pixel showed a gradual (positive) change (e.g. Figure 14B), a second showed both abrupt change in the trend component and a phenological change in the seasonal component (Figure 14C), while the third showed no change (Figure 14D). Gradual positive change spanning over the entire 2005-2009 observation period (Figure 14B) may be indicative of long term forest recovery, particularly as the EVI value (0.55) at the end of the observation period is typical of the forest class (Table 6). The second pixel (Figure14C) shows better evidence of deforestation than all the other pixels examined. There is change from low seasonal amplitude that is characteristic of the forest class to higher seasonal amplitude that is typical of croplands (Table 6). Generally, changes in the seasonal component is as a result of significant change in the phenology of the land cover, which is driven by many factors such as conversion from one land cover type to another (Verbesselt et al., 2010a;Verbesselt et al., 2010b).

Table 6: EVI values in the trend component (mean) and seasonal amplitude (mean [range]) of the land cover classes. These were computed from some randomly selected stable pixels (10 per class) in the study area

Land cover type	Trend	Seasonal amplitude
Forest	0.52	0.12 [0.08-0.18]
Cropland and cropland/vegetation mosaics	0.4	0.51 [0.25-0.8]
Other Vegetation and mosaics	0.39	0.27 [0.15-0.4]
Urban &barren	0.18	0.07 [0.04-0.09]
Water	0	0.05 [0.03-0.07]

BFAST analysis was also conducted in areas where STBM and BLSM comparison showed no deforestation and the stability test did not indicate structural change either but the PRODES data showed deforestation. Out of the 14 pixels that were examined using BFAST, 8 show no break at all (e.g. Figure 15A), 4 show abrupt change in the trend component (e.g. Figure 15B) and 2 show phenological change (e.g. Figure 15C). Again, there was some kind of recovery after the break in all the four pixels that show abrupt break in the trend component (e.g. Figure 15B), suggesting temporal forest disturbance (e.g. from fire) rather than outright deforestation (from forest clear-cut). For those pixels with phenological change, the trend component show a gentle negative or positive slope (e.g. Figure 15C) with initial and final EVI values still within the value recorded for the forest class in this study (Table 6). Also, there seems to be no appreciable difference in the seasonal amplitude before and after the phenological change was detected. Although phenological change may be indicative of change in land cover types (Verbesselt et al., 2010a;Verbesselt et al., 2010b), the failure of BLSM and STBM comparison not to capture this change could be that the forest class in this study consist of broad group of forest types (Table 1) with distinctive phenological characteristics that a transition from one type to the other may be captured by BFAST as a phenological change.

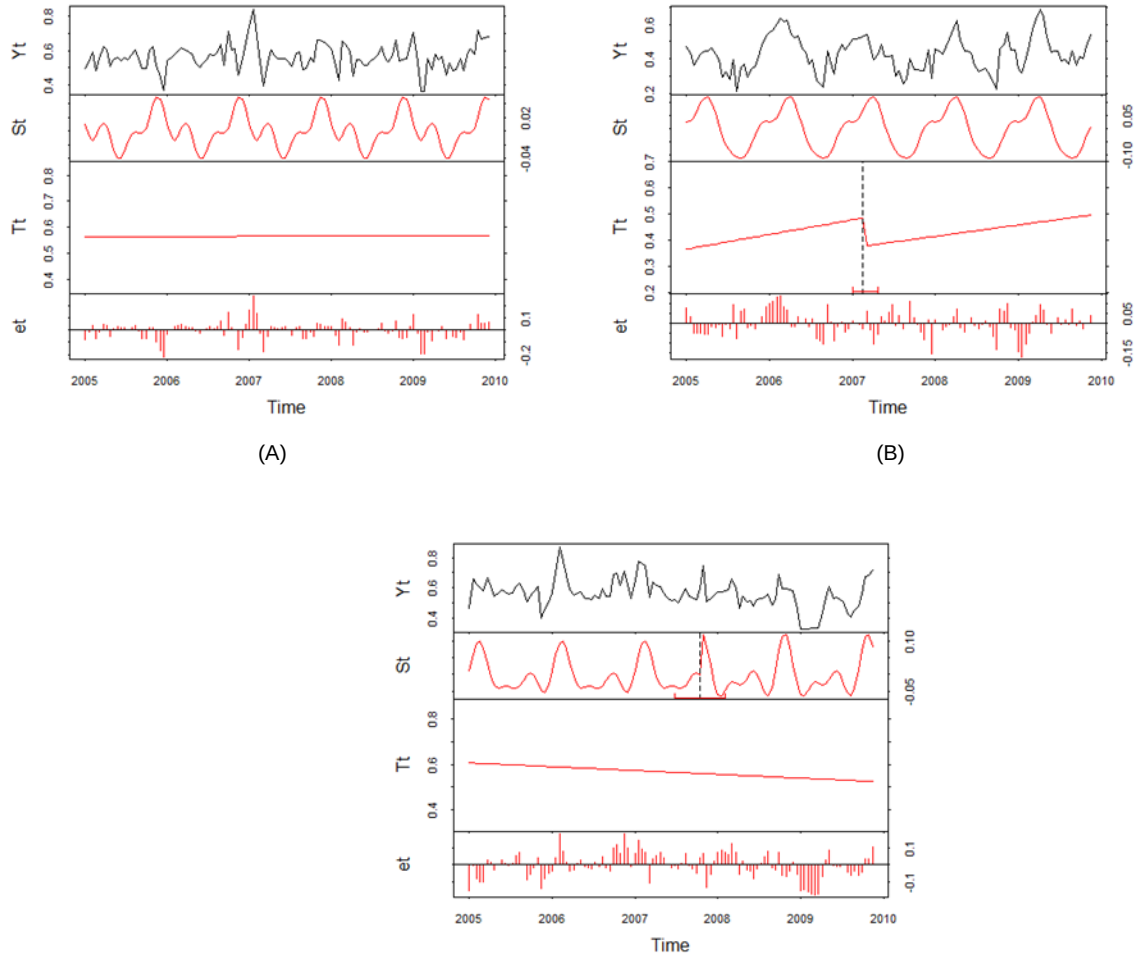

(A) (B)

(C)

Figure 15: BFAST analysis of some pixels in areas where PRODES data indicate deforestation but BLSM and STBM comparison and stability test showed no change. BFAST results show no change (A); an abrupt change in the trend component (T_t) followed by a gradual change with positive slope (B); and a phenological change in the seasonal component (S_t) with a gradual change with a negative slope in the trend component (C).

Final assessment focused on areas where BLSM and STBM comparison indicated deforestation but this was not captured by PRODES and stability test. Only three out of the 21 pixels examined showed breaks (abrupt), which were all in the trend component (e.g. Figure 16A). The abrupt break in all the three pixels were equal to or less than 0.1 EVI in magnitude, indicating relatively mild disturbance. Again, the initial and final EVI values for all three pixels are typical of the forest class (Table 6). The remaining 18 pixels showed either no change at all or a gradual change with relatively smaller and positive or negative slope (e.g. Figure 16B). Also, the EVI values are within the range characteristic of forest class. Overall, it is surprising that BLSM and STBM comparison showed deforestation when PRODES, stability test and BFAST did not generally suggest deforestation. The indicated deforestation might probably be due to classification inconsistencies between the STBM and BLSM.

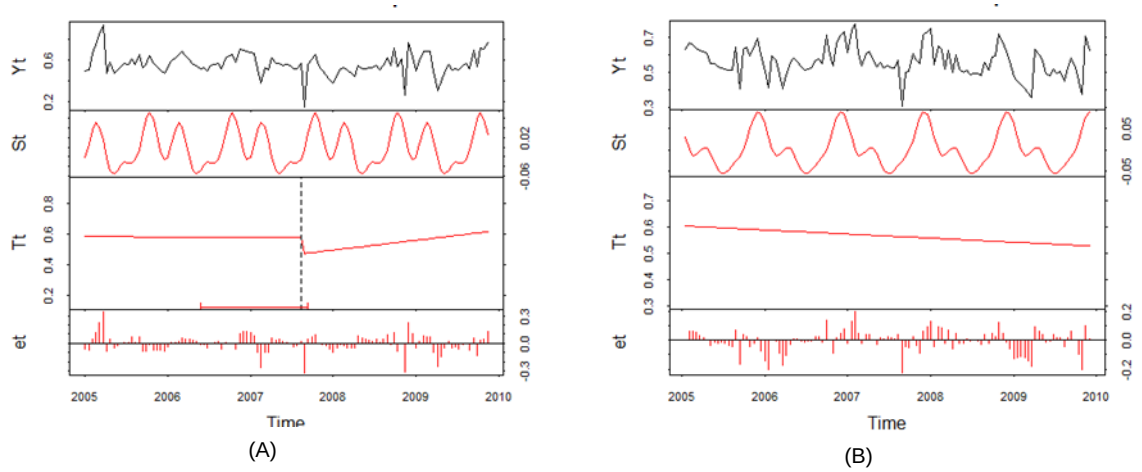

Figure 16: BFAST analysis of some pixels in areas where comparison between STBM and BLSM indicate deforestation but PRODES data and stability test showed no change. BFAST results show an abrupt change in the trend component (T_t) followed by a gradual change with positive slope (A); and a gradual change with a negative slope in the trend component (B).

4 Discussion

4.1 Can the use of multi-year satellite data and stability test produce stable 'best' land cover map with satisfactory overall- and individual class accuracies?

Accuracy assessment of the STBM produced by the multi-year and stability test approach generally yielded satisfactory overall, producer's and user's accuracies (Table 4), particularly as the computed accuracies are above the RRob target of 80 % (Bontemps et al., 2011a). Nonetheless, the producer's accuracy of the *urban and barren* class was lower (60.9 %). This can be explained by the confusion between this class and the vegetation mosaic classes (*Cropland and cropland/vegetation mosaics*, and *Other vegetation and mosaics*) (Table 4). On a larger scale, urban cores are sparsely vegetated and are easily confused with vegetation classes (Friedl et al., 2010), making large-area urban mapping problematic with the conventional mapping approach (Friedl et al., 2010;Herold et al., 2008a). Some investigators have used different approaches to map urban areas. For example, Schneider et al. (2003) incorporated information from gridded population data and DMSP (Defense Meteorological Satellite Program) night-time lights dataset to map urban areas in North America ; Schneider et al., (2010) used a stratification approach incorporating climate, vegetation, and urban topology to discriminate between urban class and other land cover types at the global scale. Incorporating one or more of these approaches to our classification scheme can improve the mapping accuracy of the *urban and barren* class.

In spite of the high accuracies of the STBM, it is important not to lose sight of the thematic detail of land cover products required by the CMC or adopted in the RRob protocol (Bontemps et al., 2011a). The RRob, for example, requires land cover maps based on two kinds of legend: the first one based on the LCCS legend (22 classes) and the second expressed in Plant Functional Types (17 classes) (Bontemps et al., 2011a). These legends are very detailed compared to the 5 class-legend adopted in this study. It is likely that the accuracy of our land cover map may decrease with increasing thematic detail as the error between classes previously grouped together may become evident and contribute to the mapping error. Nonetheless, the goal of the present study was to demonstrate the proof-of-concept of our proposed classification approach and not necessarily to create a map to be used by the CMC.

One reason that might have contributed to the high accuracy of the STBM may be linked to the source of the reference data (training and validation data). When training and validation data are obtained from the same source (as was the case in this study) the accuracy of the classified map may be a reflection of how well the classified map mirrors the reference data rather than reality. The consequence is that if the reference data is itself not error free, then the classified map may as well contain this error that can only be unmasked when it is assessed against a relatively better and independent validation data. It is better to obtain validation and training dataset from independent sources, particularly when existing data are used for accuracy assessment. Existing data are defined as reference data that are available to the accuracy assessment but at no cost, which would have

otherwise be incurred from field visits, campaign to acquire images etc. (Strahler et al., 2006). However, efforts were made in this study to combine two independent existing dataset (GlobeCover and MODIS global land cover maps). Training and validation data were sourced from areas of label agreement between both dataset. It was important to combine them in such a synergistic way because both land cover products are not free from errors.

4.2 To what extent are the class labels produced by the approach in the first research question stable over time and not affected by changes in the land cover condition?

Deforestation over 2006 and 2009 as captured by comparison between the STBM and BLSM was assessed against PRODES data with a view of assessing the stability of STBM. Our proposition is that the areas of forest in the BLSM that were not classified as forest in STBM should be as a result of deforestation. Result from the stability test showed some considerable promise in identifying land cover change or conversion as 76.1 % of areas reported as deforested by PRODES data was identified as structurally unstable by the test. Overall, the stability test showed that a large proportion (about 24 %) of the entire study area was unstable. This result corroborates reports by some studies that the region is under heavy anthropogenic and physical disturbances such as from selective logging, deforestation, forest fire, land conversion for large-scale cattle ranching and commercial agriculture (INPE, 2009;Lima et al., 2012;Morton et al., 2006). Mato Grosso, which makes up over 95 % of the study area, ranks as the leading State in Brazil with the highest deforestation rate and commercial soybean production since 2001 (Morton et al., 2006). Indicated deforestation from STBM and BLSM comparison captured a conservative 33.2 % of the deforested area that was recorded by PRODES data. BFAST analysis of areas of disagreement between PRODES data and BLSM and STBM comparison revealed that not all deforestation recorded by the PRODES data was due to outright forest clear-cut but some temporal change or disturbance, probably due to fire, drought, flooding, selective logging, or a combination of these factors. Total forest recovery from fire events and/or selective logging in this region takes only a few years, probably one or two (Souza Jr et al., 2005). It would seem logical to categorize forest undergoing these kinds of forest disturbances as a temporal change in the condition of the land cover rather than in the state of the land cover. As such forest that is under these disturbances should be classified as forest because of the inherent potential for recovery. But the use of single year data may not be suitable for such purpose, particularly if acquired when the forest is still bearing the ‘scars’ (burnt scars) from such disturbances. Unfortunately, PRODES annual estimate of deforestation is done based on information from single-date Landsat image acquired around the first of August every year (Câmara et al., 2006). This makes PRODES classification of deforestation sensitive to short-term changes in the forest cover. For areas undergoing short-term changes, our method of exploiting the full temporal information to identify unstable pixels has enabled us to classify the actual state of the land cover (forest in this case) based on the latest data, lending further credence to the usefulness of integrating multi-year data and stability test for land cover classification. This method can be used in the classification of land cover of highly variable systems.

Despite this promise, estimates of supposedly 'deforested' area from BLSM and STBM comparison was five times more than that recorded by PRODES data (subsection 3.3). This difference may partly be attributed to the differences in the total area classified as forest between PRODES data and BLSM. Visual assessment of the Brazilian portion of our study area show more areas were under forest in our thematic maps than in PRODES data. PRODES data does not consider secondary forest (or forest regrowth) (Câmara et al., 2006) and forest outside the Amazonia forest ecoregion (Arvor et al., 2012). Appreciable strips of tall, dense forest are common along stream courses in the Cerrado (savannah) ecoregion of Brazil. A corollary to this is that deforestation from secondary forest and from areas outside the Amazonia ecoregion will probably be captured by BLSM and STBM comparison and not by PRODES data. To solve this problem, some investigators (e.g. Arvor et al., 2012) have used deforestation records from other sources to compliment information from PRODES data for this region. One of such records is produced by SEMA-MT (Secretaria de Estado do Meio Ambiente, or The Secretary of State for Environment) and is based on Landsat and CBERS (China–Brazil Earth Resources Satellite program) data. However, the SEMA-MT data is not freely available like PRODES data.

Another reason that may partly be responsible for the large differences (between PRODES data and STBM and BLSM comparison) discussed above may be due to classification inconsistencies between STBM and BLSM. Some result from BFAST analysis of randomly selected pixels that showed deforestation from BLSM and STBM comparison but showed no change from PRODES data and stability test seems to indirectly support this assertion. Quite a number of the pixels examined did not show any change whether in the trend or seasonal component. Considerable differences which may not be related to land cover change can arise between two maps that have been classified using different methodologies (Friedl et al., 2010). However, there were no much differences in methodology use to create both maps except that the stability test was incorporated in the classification scheme of the STBM and data from more years was used as classification input. The spurious difference (deforestation), therefore, may have arisen due to inconsistencies in the training data. For example, there is considerable label inconsistencies between the GlobeCover 2005 and GlobeCover 2009 land cover maps which cannot be entirely attributed to land cover change (Bontemps et al., 2010). Part of the training samples for the STBM and BLSM were obtained from GlobeCover 2009 and 2005 respectively. It was likely that the inconsistencies between the GlobeCover maps may have propagated to our maps also. Also, classification inconsistencies may also be due to the problem of mixed pixel. At 250 m spatial resolution, the MODIS image can contain different classes in heterogeneous areas of the landscape. The class label for a mixed pixel may toggle time-to-time between two or more classes contained in that pixel (Friedl et al., 2010). Thus, due to the problem of mixed pixel associated with coarse resolution images, it might be difficult to totally eradicate the problem of label instability in coarse resolution maps. For example, Using a 500 m spatial resolution MODIS images, Friedl et al. (2010) were only able to reduce the proportion of pixels with spurious

inter-annual change (at the global level) from 30 % to 10 % in a classification scheme designed to solve the problem of label instability.

5 Conclusion and further work

Stable and accurate land cover maps, particularly for large areas— ranging from regional to global scale—, are recently being demanded by a number of user communities such as the CMC. Unfortunately, the conventional mapping approach of using single year data to map land cover at the global scale makes these maps sensitive to intra- and inter-annual variation in the condition of the land cover. Uncertainties as to the correct state of the land cover can propagate through applications that utilize these land cover maps. As one of 11 ECVs, reliable and accurate information on the state and dynamics of land cover is pivotal to our understanding of the climate system.

Here we propose a novel approach in large-area land cover classification that uses multi-year satellite data and stability test to produce stable 'best' land cover map (STBM) that should be accurate and less sensitive to the variation in the land cover condition. The assumption of using multi-year satellite data is that the land cover will be mapped in a consistent way over time if there is no change in the state of the land cover. Prior to land cover classification, the stability test is used to differentiate pixels that are unstable (probably due to change) from those that are stable over the observation period. Stable pixels are classified with the multi-year satellite data while unstable pixels are classified with the latest year data. This concept was tested using 5 years (2005-2009) MODIS satellite data acquired over a region encompassing the State of Mato Grosso and extending marginally into Eastern Bolivia.

Results of the stability test performed on the EVI band showed that about 24 % of the study area was unstable over the observation period. This corroborates reports by some organizations and investigators that the area is under heavy disturbance. There was good agreement between the stability test and PRODES data as 76.1 % of areas considered deforested by PRODES was captured as unstable by the stability test.

Our first research objective concerns the accuracy of the classification output using our propose approach to land cover mapping. Results from this study demonstrate that satisfactory overall and individual class accuracies of land cover classified by the integration of multi-year satellite data and stability test is feasible. Generally, the overall and individual class accuracies of the STBM exceeded the threshold target (80 %) considered satisfactory by the ESA CCI-LC RRob protocol (Bontemps et al., 2011a). However, the thematic detail of the STBM is far less than the specification by the ESA-CCI RRob. The mapping accuracy of our approach will need to be tested using more detailed thematic legend such as the LCCS and PFT. The LCCS and PFT are among the most detailed legends used in large area land cover mapping.

As a second research objective, we evaluated the robustness of our approach to produce stable labels by comparing indicated deforestation from comparing STBM and a baseline status map (BLSM) against deforestation from PRODES data. Result from our study showed that only 33.2 % of areas captured as deforested by PRODES was also indicated as deforested by STBM and BLSM comparison. Pixels were randomly selected from areas of disagreement. These pixels were analysed

using BFAST. The result of the analysis showed that PRODES data confounds short term forest disturbances (e.g. from drought, fire and selective logging) as deforestation in most of the areas where STBM and BSLM comparison did not indicate deforestation. In this regard, our approach was able to identify forest pixels that were disturbed (but not converted to other land cover types) as unstable and then classify the pixels using the latest year data. We were able to classify the true state of the land cover (forest) because the forest may have fully recovered from the disturbance by the latest year. BFAST analysis also revealed that some indicated deforestation from comparison STBM and BSLM were not deforestation. We attributed this to classification inconsistences, particularly as the training data were obtained from land cover maps (GlobeCover and MODIS) that are known to contain some errors. Also, the problem of mixed pixel associated with coarse resolution image (250 m in our case) may also have contributed to classification inconsistencies. Classification label for a mixed pixel may vary from time-to-time between two or more classes in the pixel.

Overall, there is considerable promise that the approach can reduce the sensitivity of the classification output to variation in the land cover condition. However, further work needs to be done to improve the effectiveness of our proposed approach to overcome the present problem of label instability inherent in current land cover maps. This work can build on the gains from this study and correct some of its limitations as detailed below:

1. A pixel time series was selected for stability test analysis when it lacked less than 40 % of the data. Most studies used lower and more stricter threshold such as 10 % (Verbesselt et al., 2010b), 15 % (Verbesselt et al., 2012) and 20 % (Beurs and Henebry, 2010). Although we assumed that the OLS-fitting of the harmonic-seasonal model can cope with missing data, the regression parameters can only be estimated consistently when there is at least one observation at certain frequencies (Verbesselt et al., 2012). The 40 % threshold adopted in this study may impact the reliability of the estimated structural change, particularly if the gaps in the time series are wider and exceeded the frequencies of our lower harmonic terms (especially the third component of the seasonal harmonic term). In conducting stability test in a region affected by persistent cloud like the one in this study, there is a trade-off between the need to increase the reliability of the stability test by using a low and stricter threshold for missing data and the need to include as much pixels in the analysis by using a high threshold.

2. In this study, unstable pixels (from stability test) were all classified with the latest year data (2009). The classification output (class label) using single year data may reflect land cover condition instead of the land cover state. The stability test can be optimised to detect both change (instability) and the timing of the change. In this regard, we can leverage concepts from methods such as BFAST that are used to detect place and time of change in ecosystem from satellite time series. With this improvement to our stability test, unstable pixels should be classified using data from the date of the last detected change and onwards. By doing so, unstable pixels that were disturbed earlier in the observation period can be classified with

more data, possibly more than one year data. This will increase the chances of classifying the actual state of the land cover of the unstable pixels.

3. Assessing label stability of a land cover map requires accurate and reliable land cover change data. In this study, the PRODES data used to assess deforestation is not totally accurate in the temporal dimension as forest regrowth (or secondary forest) is not considered by PRODES data. Relying on such data like PRODES for stability assessment may be misleading.

4. There is need to use accurate and reliable reference data (training and validation data) for the classification scheme. Where possible, the use of existing data such as maps should be avoided because they may not be totally free from errors. But where the use of existing data as reference source cannot be avoided, the resolution of the existing data should be the same or higher than the imagery that will be classified. The reference data used in our study are of lower resolution than our image; the problem of mixed pixel associated with low resolution maps can give misleading result.

5. There is need to further test our classification approach in other ecological regions of the world, preferably where cloud disturbances are minimal. This will allow for the utilization of the full temporal information of the time series for land cover classification. This was not the case in this study as input features for classification are limited to the periods of the year when there is less cloud cover in the region.

6 References

Arozarena, A., Villa, G., Valcarcel, N., Peces, J. J., Domenech, E., and Porcuna, A.: New concept on land cover/land use information system in Spain. Desing and production, Proceedings of the 2nd Workshop of the EARSeL SIG on Land Use and Land Cover, Centre for Remote Sensing of Land Surfaces, Bonn, Germany, 2006, 215–223,

Arvor, D., Meirelles, M., Dubreuil, V., Bégué, A., and Shimabukuro, Y. E.: Analyzing the agricultural transition in Mato Grosso, Brazil, using satellite-derived indices, Applied Geography, 32, 702-713, 2012.

Bartholomé, E., and Belward, A. S.: GLC2000: A new approach to global land cover mapping from earth observation data, Int. J. Remote Sens., 26, 1959-1977, 10.1080/01431160412331291297, 2005.

Beurs, K. M. d., and Henebry, G. M.: A land surface phenology assessment of the northern polar regions using MODIS reflectance time series, Canadian Journal of Remote Sensing, 36, S87-S110, 10.5589/m10-021, 2010.

Bontemps , S., Defourney, P., Van Bogaert, E., Kalogirou, V., and Arino, O.: GlobCover 2009:Products description and validation report, ESA GlobCover project, http://ionia1.esrin.esa.int/, 2010.

Bontemps, S., Brockman, C., Defourney, P., Kirches, G., and Martin, B.: CCI Land Cover project – Round-Robin Protocol , version 1.2, www.esa-landcover-cci.org, 2011a.

Bontemps, S., Herold, M., Kooistra, L., Van Groenestijn, A., Hartley, A., Arino, O., Moreau, I., and Defourny, P.: Revisiting land cover observations to address the needs of the climate modelling community, Biogeosciences Discuss., 8, 7713-7740, 10.5194/bgd-8-7713-2011, 2011b.

Brown, I. F., Schroeder, W., Setzer, A., de Los Rios, M. M., Pantoja, N., Duarte, A., and Marengo, J.: Monitoring fires in southwestern Amazonia rain forests, Eos, 87, 253-255, 2006.

Câmara, G., Valeriano, D. M., and Soares, J. V.: Metodologia para o cálculo da taxa anual de desmatamento na Amazônia Legal, São José dos Campos: Inpe, 2006.

Congalton, R. G., and Green, K.: Assessing the accuracy of remotely sensed data : principles and practices, Lewis Publications, Boca Raton, FL, 1999.

De Fries, R. S., Hansen, M., Townshend, J. R. G., and Sohlberg, R.: Global land cover classifications at 8 km spatial resolution: The use of training data derived from Landsat imagery in decision tree classifiers, Int. J. Remote Sens., 19, 3141-3168, 1998.

de Jong, R., Verbesselt, J., Schaepman, M. E., and de Bruin, S.: Trend changes in global greening and browning: Contribution of short-term trends to longer-term change, Global Change Biology, 18, 642-655, 2012.

Defourny, P., Bicheron, P., Brockman, C., Bontemps, S., van Bogaert, E., Vancutsem, C., Pekel, J. F., Huc, M., Henry, C., Ranera, F., Achard, F., Di Gregorio, A., Herold, M., Leroy, M., and Arino, O.: The first 300 m global land cover map for 2005 using Envisat MERIS time series: a product of the GlobCover system, Proceedings of the 33rd International Symposium on Remote Sensing of Environment, Stresa, Italy, 2009,

Defourny, P., Bontemps , S., Martin, B., Brockman, C., Fomferra, N., Grit, K., and Kruger, O.: CCI Land Cover project – Product Specification Document, version 1.2, www.esa-landcover-cci.org 2011.

Defries, R. S., and Townshend, J. R. G.: NDVI-derived land cover classifications at a global scale, Int. J. Remote Sens., 15, 3567-3586, 1994.

Di Gregorio, A.: Land cover classification system : classification concepts and user manual : LCCS, Food and Agriculture Organization of the United Nations, Rome, 2005.

EEA – European Environment Agency: Corine Land Cover 2006 raster data, www.eea.europa.eu/data-and-maps/data/corine-land-cover-2006-raster, 2009.

EEA – European Environment Agency: Corine Land Cover 2000 raster data (version 13), www.eea.europa.eu/data-and-maps/data/corine-land-cover-2000-raster, 2010a.

EEA – European Environment Agency: Corine Land Cover 1990 raster data (version 13), www.eea.europa.eu/data-and-maps/data/corine-land-cover-1990-raster, 2010b.

ESA – European Space Agency: ESA Climate Change Initiative description, EOP-SEP/TN/0030-09/SP, http://earth.eo.esa.int/workshops/esa_cci/ESA_CCI_Description.pdf, 2009.

FAO – Food and Agriculture Organization of the United Nations: Africover databases on environmental resources, FAO, www.africover.org, 2003.

Foody, G. M.: Status of land cover classification accuracy assessment, Remote Sens. Environ., 80, 185-201, 2002.

Friedl, M. A., McIver, D. K., Hodges, J. C. F., Zhang, X. Y., Muchoney, D., Strahler, A. H., Woodcock, C. E., Gopal, S., Schneider, A., Cooper, A., Baccini, A., Gao, F., and Schaaf, C.: Global land cover mapping from MODIS: Algorithms and early results, Remote Sens. Environ., 83, 287-302, 10.1016/s0034-4257(02)00078-0, 2002.

Friedl, M. A., Sulla-Menashe, D., Tan, B., Schneider, A., Ramankutty, N., Sibley, A., and Huang, X.: MODIS Collection 5 global land cover: Algorithm refinements and characterization of new datasets, Remote Sens. Environ., 114, 168-182, 10.1016/j.rse.2009.08.016, 2010.

GCOS – Global Climate Observing System: Implementation plan for the Global Observing System for Climate in Support of the UNFCCC, World Meteorological Organisation, www.wmo.int/pages/prog/gcos/Publications/gcos-138.pdf, August 2010 (update).

Ge, J., Torbick, N., and Qi, J.: Biophysical evaluation of land-cover products for land-climate modeling, Earth Interactions, 13, 2009.

Geerken, R. A.: An algorithm to classify and monitor seasonal variations in vegetation phenologies and their inter-annual change, ISPRS Journal of Photogrammetry and Remote Sensing, 64, 422-431, 2009.

Hansen, M. C., Defries, R. S., Townshend, J. R. G., and Sohlberg, R.: Global land cover classification at 1 km spatial resolution using a classification tree approach, Int. J. Remote Sens., 21, 1331-1364, 2000.

Herold, M., Mayaux, P., Woodcock, C. E., Baccini, A., and Schmullius, C.: Some challenges in global land cover mapping: An assessment of agreement and accuracy in existing 1 km datasets, Remote Sens. Environ., 112, 2538-2556, 2008a.

Herold, M., Schmullius, C., and Arino, O.: Building saliency, legitimacy, and credibility towards operational global land cover observations, European Space Agency, (Special Publication) ESA SP, 2008b,

Herold, M., Woodcock, C., Cihlar, M., Wulder, M., Arino, O., Achard, F., Hansen, M., Olsson, H., Schmulllius, C., Brady, M., Di Gregorio, A., Latham, J., and Sessa, R.: Assessment of the status of the development of the standards for the Terrestrial Essential Climate Variables: T9 Land Cover, FAO, www.fao.org/gtos/doc/ECVs/T09/T09.pdf, 2009.

Herold, M., van Groenestijn, A., Kooistra, L., Kalogirou, V., and Arino, O.: CCI Land Cover project – User Requirements Document, version 2.2, www.esa-landcover-cci.org, 2011.

Huete, A., Didan, K., Miura, T., Rodriguez, E. P., Gao, X., and Ferreira, L. G.: Overview of the radiometric and biophysical performance of the MODIS vegetation indices, Remote Sens. Environ., 83, 195-213, 2002.

Hüttich, C., Herold, M., Wegmann, M., Cord, A., Strohbach, B., Schmullius, C., and Dech, S.: Assessing effects of temporal compositing and varying observation periods for large-area land-cover mapping in semi-arid ecosystems: Implications for global monitoring, Remote Sens. Environ., 115, 2445-2459, 10.1016/j.rse.2011.05.005, 2011.

INPE-Instituto Nacional de Pesquisas Espaciais (Brazilian Space Agency): Desmatamento anual na Amazônia Legal, 2009.

Kuan, C.-M., and Hornik, K.: The generalized fluctuation test: A unifying view, Econometric Reviews, 14, 135-161, 10.1080/07474939508800311, 1995.

Lima, A., Silva, T. S. F., de Aragão, L. E. O. C., de Feitas, R. M., Adami, M., Formaggio, A. R., and Shimabukuro, Y. E.: Land use and land cover changes determine the spatial relationship between fire and deforestation in the Brazilian Amazon, Applied Geography, 34, 239-246, 2012.

Loveland, T. R., Reed, B. C., Brown, J. F., Ohlen, D. O., Zhu, Z., Yang, L., and Merchant, J. W.: Development of a global land cover characteristics database and IGBP DISCover from 1 km AVHRR data, Int. J. Remote Sens., 21, 1303-1330, 2000.

Maxwell, S. K., Hoffer, R. M., and Chapman, P. L.: AVHRR composite period selection for land cover classification, Int. J. Remote Sens., 23, 5043-5059, 10.1080/01431160210145579, 2002.

Morton, D. C., DeFries, R. S., Shimabukuro, Y. E., Anderson, L. O., Arai, E., Del Bon Espirito-Santo, F., Freitas, R., and Morisette, J.: Cropland expansion changes deforestation dynamics in the southern Brazilian Amazon, Proceedings of the National Academy of Sciences of the United States of America, 103, 14637-14641, 2006.

Richards, J. A., and Jia, X.: Remote sensing digital image analysis : an introduction, Springer, Berlin; Heidelberg; New York, 2006.

Ronald Eastman, J., Sangermano, F., Ghimire, B., Zhu, H., Chen, H., Neeti, N., Cai, Y., Machado, E. A., and Crema, S. C.: Seasonal trend analysis of image time series, Int. J. Remote Sens., 30, 2721-2726, 10.1080/01431160902755338, 2009.

Schneider, A., Friedl, M. A., McIver, D. K., and Woodcock, C. E.: Mapping urban areas by fusing multiple sources of coarse resolution remotely sensed data, Photogrammetric Engineering and Remote Sensing, 69, 1377-1386, 2003.

Schneider, A., Friedl, M. A., and Potere, D.: Mapping global urban areas using MODIS 500-m data: New methods and datasets based on 'urban ecoregions', Remote Sens. Environ., 114, 1733-1746, 2010.

Shimabukuro, Y. E., Batista, G. T., Mello, E. M. K., Moreira, J. C., and Duarte, V.: Using shade fraction image segmentation to evaluate deforestation in Landsat Thematic Mapper images of the Amazon Region, Int. J. Remote Sens., 19, 535-541, 1998.

Souza Jr, C. M., Roberts, D. A., and Cochrane, M. A.: Combining spectral and spatial information to map canopy damage from selective logging and forest fires, Remote Sens. Environ., 98, 329-343, 10.1016/j.rse.2005.07.013, 2005.

Strahler, A., Boschetti, L., Foody, G., Friedl, M., Hansen, M., Herold, M., Mayaux, P., Morisette, J., Stehman, S., and Woodcock, C.: Global land cover Validation: recommendations for evaluation and accuracy assessment of global land cover maps, Office for Official Publications of the European Communities, 1-51 pp., 2006.

Verbesselt, J., Hyndman, R., Newnham, G., and Culvenor, D.: Detecting trend and seasonal changes in satellite image time series, Remote Sens. Environ., 114, 106-115, 2010a.

Verbesselt, J., Hyndman, R., Zeileis, A., and Culvenor, D.: Phenological change detection while accounting for abrupt and gradual trends in satellite image time series, Remote Sens. Environ., 114, 2970-2980, 2010b.

Verbesselt, J., Zeileis, A., and Herold, M.: Near real-time disturbance detection using satellite image time series, Remote Sens. Environ., 123, 98-108, 2012.

Verger, A., Baret, F., and Weiss, M.: A multisensor fusion approach to improve LAI time series, Remote Sens. Environ., 115, 2460-2470, 2011.

Wagenseil, H., and Samimi, C.: Assessing spatio-temporal variations in plant phenology using Fourier analysis on NDVI time series: results from a dry savannah environment in Namibia, Int. J. Remote Sens., 27, 3455-3471, 10.1080/01431160600639743, 2006.

Walker, R.: The scale of forest transition: Amazonia and the Atlantic forests of Brazil, Applied Geography, 32, 12-20, 2012.

Xu, M., Watanachaturaporn, P., Varshney, P. K., and Arora, M. K.: Decision tree regression for soft classification of remote sensing data, Remote Sens. Environ., 97, 322-336, 2005.

Zeileis, A., Leisch, F., Hornik, K., and Kleiber, C.: Strucchange: An R package for testing for structural change in linear regression models, Journal of Statistical Software, 7, 1-38, 2002.

Zeileis, A., Shah, A., and Patnaik, I.: Testing, monitoring, and dating structural changes in exchange rate regimes, Computational Statistics and Data Analysis, 54, 1696-1706, 2010.